*J. Fluid Mech.* (1980), *vol.* 98, *part* 3, *pp.* 555–585
*Printed in Great Britain*



# On coastal trapped waves at low latitudes in a stratified ocean

By J. S. ALLEN AND R. D. ROMEA
School of Oceanography, Oregon State University, Corvallis, Oregon 97331

(Received 15 May 1978 and in revised form 10 October 1979)

Results from idealized ocean models indicate that equatorially trapped baroclinic waves incident on an eastern boundary may be partially transmitted north and south along the coast as boundary-trapped internal Kelvin waves. The offshore scale of the coastal internal Kelvin waves is the internal Rossby radius of deformation $\delta_R$, which decreases as the Coriolis parameter $f$ increases. The effect of the presence of a continental slope of width $L_s$, along a north–south oriented coastline, on the poleward propagation of coastal trapped internal Kelvin waves is studied in a two-layer $\beta$-plane model. The waves propagate from regions near the equator where $\delta_R > L_s$ to mid-latitudes where $\delta_R < L_s$. It is assumed that $f$ varies slowly on the alongshore scale of the waves $L$, that $L \gg L_s$, and that either the topographic slope is weak or that the upper-layer depth is small compared to the lower-layer depth. All of the coastal trapped waves present in the model are non-dispersive. For most values of $f$, the cross-shelf eigenfunctions consist of the internal Kelvin wave and an infinite set of continental shelf waves whose vertical structure depends on $\delta_R/L_s$. For $\delta_R/L_s \gg 1$, the shelf waves are bottom trapped while for $\delta_R/L_s \ll 1$ they are barotropic. The wave speeds $c_n$ of the shelf waves vary linearly with $f$, whereas the wave speed $c_0$ of the internal Kelvin wave is independent of $f$. As $f$ increases through critical values $f_{Cn}$, where $c_n$ approaches $c_0$, the phase speeds and the eigenfunctions vary so that the eigenfunctions represent a different type of wave on either side of $f_{Cn}$. In the slowly-varying approximation, the alongshore energy flux in each eigenfunction is a constant. It follows that an internal Kelvin wave which has a wavelength short enough that the slowly-varying approximation remains valid and which propagates poleward from the equatorial region where $f < f_{C1}$ will transform into a shelf wave, at values of $f$ near $f_{C1}$, and will continue propagation poleward in that form. As a result, coastal trapped baroclinic disturbances may be able to propagate efficiently from the equatorial region to mid-latitudes where they may take the form of barotropic shelf waves.

## 1. Introduction

An important dynamical property of linear, inviscid, time-dependent, stratified ocean models is the possible existence of equatorially trapped baroclinic wave motions (e.g. Moore & Philander 1977). These waves play a major role in studies of the unsteady response of the tropical ocean to meteorological forcing (e.g. Lighthill 1969; Cane & Sarachik 1976, 1977; Moore & Philander 1977). On an equatorial $\beta$-plane, with $x$, $y$ co-ordinates in the zonal and meridional directions, respectively, and with Coriolis parameter $f = \beta y$, the latitudinal trapping scale of these waves is the baroclinic

0022-1120/80/4455-1090 $02.00 

equatorial radius of deformation, $\delta_{En} = (gH_{en}/\beta^2)^{\frac{1}{4}}$, where $g$ is the acceleration of gravity and $H_{en}$ is the equivalent depth for the $n$th vertical baroclinic mode. An approximate value of $\delta_{E1}$ for a two-layer model of the eastern equatorial Pacific ocean is $\delta_{E1} \simeq 260\,\mathrm{km}$ and the characteristic wave speed is $c_E^{(1)} = (gH_{e1})^{\frac{1}{2}} \simeq 160\,\mathrm{cm\,s^{-1}}$ (appendix B).

The behaviour of oceanic equatorially trapped waves, both in free and in forced situations, is strongly affected by the presence of meridional boundaries. In particular, Moore (1968) (see Moore & Philander 1977) has shown that equatorially trapped free waves at a single frequency incident on an eastern boundary may be partially reflected back into the equatorial wave guide and partially transmitted north and south along the coast as boundary-trapped internal Kelvin waves. The specific process of the transmission of disturbances along an eastern boundary after the incidence of an equatorial Kelvin wave has been studied by Anderson & Rowlands (1976) (see also Cane & Sarachik 1977). The ability of baroclinic disturbances, following generation by wind stress fluctuations over the equatorial Pacific Ocean, to propagate as free waves eastward along the equator and subsequently north and south along the coast of South America plays an important part in recent theoretical and numerical models of El Niño† (McCreary 1976; Hurlburt, Kindle & O'Brien 1976).

In addition to the theoretical model results, there is recent observational evidence for the poleward propagation of velocity fluctuations along the coast of South America. Measurements of currents on the continental shelf and slope in the coastal upwelling region off Peru between 10° S and 15° S by the CUEA (Coastal Upwelling Ecosystems Analysis) program in 1976 and 1977, show that fluctuations in the alongshore velocity field, which are baroclinic over the slope, generally propagate poleward non-dispersively with a speed of approximately $230\,\mathrm{cm\,s^{-1}}$ (Smith 1978; see also Brink, Allen & Smith 1978). The fluctuations in the alongshore velocity component are, in general, poorly correlated with the local alongshore component of the wind stress, in contrast to other upwelling regions, and, therefore, are presumably caused by mechanisms other than local or nearby coastal winds. The forcing mechanism for these disturbances is not known at the present, but one candidate for the region of their origin is the equatorial waveguide.

The present study is motivated primarily by a desire to understand coastal wave propagation processes which may be important at low latitudes off the Pacific coast of South America.

In all of the above-mentioned theoretical and numerical studies on the interaction of equatorially trapped wave motions with eastern boundaries, the ocean model has a flat bottom and the boundary is represented by a vertical wall. For incident equatorial waves at a single frequency, the coastal trapped waves that result, away from the equatorial region, are flat-bottom internal Kelvin waves (Moore 1968). These waves propagate poleward along the coast non-dispersively with wave speed $c^{(n)} = (gH_{en})^{\frac{1}{2}}$ and with a small inclination of the phase lines relative to the coast due to the $\beta$ effect. The offshore scale is given by the internal Rossby radius of deformation $\delta_{Rn} = c^{(n)}/f$. Near the equator ($f \to 0$, $\delta_{Rn} \to \infty$), the internal-Kelvin-wave region merges with the

† El Niño is the name given to a phenomenon which involves the appearance of anomalously warm surface water off the coast of South America near the equator, specifically off Ecuador and Peru. This condition may persist for a year or more. During the occurrence of El Niño events there have been large declines in the catch of the Peru anchovy fishery.

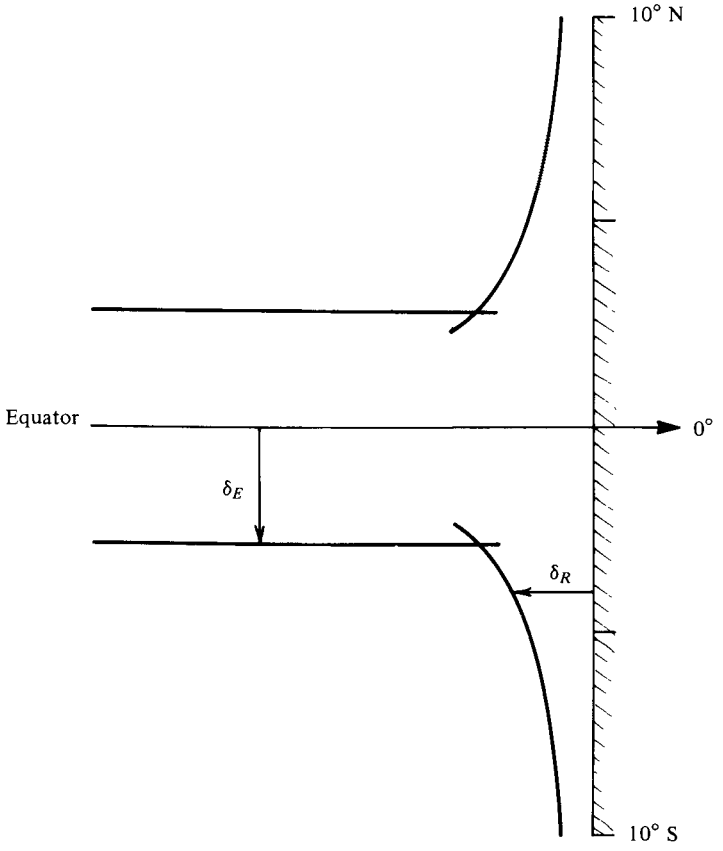


FIGURE 1. Schematic diagram of the equatorial ocean and an eastern boundary showing the regions encompassed by the equatorial Rossby radius of deformation $\delta_E$ and the boundary Rossby radius of deformation $\delta_R$, for the first baroclinic mode.

equatorial waveguide as shown in figure 1. The wave speed $c^{(1)}$ of the first baroclinic-mode internal Kelvin wave in the region of interest off South America, for example between 5° and 10° S, is approximately $c^{(1)} \simeq 100\,\mathrm{cm\,s^{-1}}$ (appendix B).

In reality, of course, the eastern boundary is not a vertical wall, but is composed of a continental shelf and slope. If the width of the shelf–slope region is small compared to the relevant offshore scale of the waves, it might be expected that the presence of the continental slope would have a minor effect on the wave reflexion and transmission processes. The width of the continental margin off the Pacific coast of South America is variable. An estimate, from bathymetric charts, of the distance $L_s$ over which the depth increases offshore from roughly 180 m to 3650 m, i.e. from 100 to 2000 fathoms, is given as a function of latitude in table 1. Also included in that table is the variation with latitude of the Rossby radius of deformation for the first baroclinic mode $\delta_R (= \delta_{R1} = c^{(1)}/f)$. From table 1, we see that $\delta_R$ is generally larger than $L_s$ from 0° to 6° S and that it is substantially larger than $L_s$ from 0° to 3°. As the latitude increases, $\delta_R$ decreases so that, for latitudes higher than 6° S, $\delta_R < L_s$.

A horizontal spatial scale for the bottom topography of the continental margin, which is dynamically more important than $L_s$ for coastal trapped waves (Allen 1975),

| Latitude (° S) | $L_s$ (km) | $\delta'_B$ (km) | $\delta'_R$ (km) | $c'_1$ (cm s$^{-1}$) |
|---|---|---|---|---|
| 0 | 46 | 15 | — | 0 |
| 1 | 33 | 11 | 394 | 4 |
| 2 | 42 | 14 | 197 | 9 |
| 3 | 60 | 20 | 131 | 20 |
| 4 | 75 | 25 | 99 | 33 |
| 5 | 40 | 13 | 79 | 22 |
| 6 | 46 | 15 | 66 | 30 |
| 7 | 57 | 18 | 56 | 43 |
| 8 | 95 | 31 | 49 | 82 |
| 9 | 79 | 26 | 44 | 77 |
| 10 | 77 | 25 | 40 | 84 |
| 11 | 107 | 35 | 36 | 127 |
| 12 | 101 | 33 | 33 | 131 |
| 13 | 100 | 33 | 31 | 140 |
| 14 | 55 | 18 | 28 | 83 |
| 15 | 55 | 18 | 27 | 89 |
| 16 | 68 | 22 | 25 | 117 |
| 17 | 97 | 32 | 24 | 177 |
| 18 | 110 | 36 | 22 | 212 |
| 19 | 110 | 36 | 21 | 224 |
| 20 | 96 | 32 | 20 | 205 |

TABLE 1. Parameter values off the Pacific coast of South America. $L_s$ is the shelf–slope width between depths of 180 m and 3650 m, i.e. between 100 and 2000 fathoms. $\delta'_B$ is an estimated characteristic scale length of the shelf–slope bottom topography (appendix B). $\delta'_R$ is the internal Rossby radius of deformation of the first baroclinic mode. $c'_1$ is the estimated wave speed of the first continental shelf wave (appendix B). The primes on $\delta'_B$, $\delta'_R$ and $c'_1$ denote dimensional values consistent with the notation starting in § 2.

is the scale length $\delta_B = H/H_x$, where $x$ is the co-ordinate normal to the coast, $H(x)$ is the depth, and the subscript $x$ denotes differentiation. Utilizing a rough estimate, such as $\delta_B \simeq L_s H/\Delta H$, we see, however, that an approximate characteristic value of $\delta_B$ is linearly related to $L_s$ and is generally some fraction ( $< 1$) of $L_s$, for example for a linear slope $\delta_B \simeq 1/2L_s$. Estimated values of $\delta_B$ for the South American coast (appendix B) are also given in table 1.

For an internal Kelvin wave it may be expected (Allen 1975; see also the latter part of appendix A) that, when $\delta_R$ decreases to the point where it has a magnitude similar to $\delta_B$, effects from the bottom topography of the continental slope will be as important as those from the density stratification. When that is the case, the internal-Kelvin-wave structure should be modified into that of a more general coastal trapped-wave mode (Allen 1975; Wang & Mooers 1976). If the structure of the mode remains dominantly that of an internal Kelvin wave, however, the waves will be confined to a distance approximately $\delta_R$ from the coast. If that is the case, the waves could possibly propagate poleward to regions where the offshore scale $\delta_R \ll L_s$.

It seems doubtful that, when $\delta_R \ll L_s$, substantial amounts of energy can propagate large distances along the coast. This statement is motivated by observations off Oregon at 45° N in the summers of 1972 and 1973 (Kundu & Allen 1976) where, in spite of the presence of strong stratification on the shelf, solid indications of a alongshore propagation in internal Kelvin-type wave modes have not been found. In contrast, there is

considerable evidence from the same location (Huyer *et al.* 1975; Kundu & Allen 1976) for alongshore propagation of velocity fluctuations primarily in the form of barotropic continental shelf waves. It is possible that the propagation of baroclinic disturbances at mid-latitudes, where the offshore scale $\delta_R \simeq 10$–$15\,\mathrm{km}$ generally covers a small region over the continental shelf, is adversely affected by large inhomogeneities in the density field, by the relatively large mean currents observed near the coast, or by the irregular bottom topography of the continental shelf.

We have a situation, therefore, where baroclinic disturbances in the form of coastal trapped internal Kelvin waves, which originate in the equatorial region, play an important role in flat bottom theoretical models of the response of the eastern Pacific Ocean. We also have recent observational evidence for the poleward propagation of velocity fluctuations, which are evidently not related to local winds, off Peru. On the other hand, theoretical results indicate that the structure of an internal-Kelvin-wave mode should change as it propagates poleward along a coast with a continental shelf and slope. In addition, at mid-latitudes, observations and physical arguments indicate that baroclinic disturbances, if they are in a form similar to internal Kelvin waves, are unlikely to propagate efficiently over large distances alongshore. As a consequence, the following question naturally arises. If, in a real ocean with a continental slope on the eastern boundary, there are baroclinic disturbances generated in the equatorial region and transmitted poleward along the coast as internal Kelvin waves, what is the fate of this wave motion as $f$ increases and the offshore scale $\delta_R$ decreases?

To gain insight into the answer to the above question, we study the behaviour at low latitudes of coastal trapped waves in a stratified ocean with a continental shelf and slope and with a variable Coriolis parameter. The simplest possible model which retains the essential physics is utilized. We consider a two-layer model on a $\beta$-plane (away from the immediate vicinity of the equator) with an idealized continental shelf and slope along a north–south oriented eastern boundary. The bottom topography is assumed to vary only in the onshore–offshore (east–west) direction $x$, and is independent of the alongshore (north–south) co-ordinate $y$. It is further assumed that the alongshore scale of variation of the waves $\delta_y = L$ is much larger than the shelf-slope width $L_s$, i.e. $L \gg L_s$. As a result, all of the coastal trapped waves in the model are non-dispersive and the mathematics is considerably simplified. The Coriolis parameter $f(y)$ is assumed to vary slowly on the alongshore scale $L$ of the waves. The effect of the variation of $f$ is treated by perturbation methods for slowly varying waveguides in a manner somewhat similar to that used by Miles (1972) for external Kelvin waves and by Grimshaw (1977) for barotropic continental shelf waves.

## 2. Formulation

We consider a two-layer model on a $\beta$-plane for the northern hemisphere. Cartesian co-ordinates $(x', y', z')$ are utilized† with $x'$ positive *westward*, $y'$ positive *southward*, and $z'$ positive vertically upward. The Coriolis parameter $f'$ is a function of $y'$, i.e. $f' = f'(y')$, with $df'/dy' = -\beta'$. Stratification is modelled by two layers of homogeneous fluids of different density, with the heavier fluid on the bottom. The top surface is

† In this and the following sections, dimensional variables, for which a non-dimensional counterpart will be defined, are denoted with primes. Note that, in the abstract and in § 1, dimensional variables are not denoted with primes.

bounded by a horizontal rigid lid. The upper-layer fluid has density $\rho_1$ and a constant undisturbed depth $H_1'$. The lower-layer fluid has density $\rho_2$ and, in general, a variable undisturbed depth $H_2' = H_2'(x', y')$. The total depth is $H' = H_1' + H_2'$. The difference in density $\Delta\rho = \rho_2 - \rho_1$ is assumed to be small, $\Delta\rho \ll \rho_2$.

The fluid is bounded on the east by a straight, north–south-oriented coastline at $x' = 0$. Along this boundary there is a continental shelf and slope topography which is independent of $y'$ and which is confined to the region $0 \leqslant x' \leqslant L_s$. The depth is constant, $H' = H_0'$, in the interior region $x' \geqslant L_s$. The undisturbed lower-layer depth in this region is $H_{20}'$, i.e. $H_0' = H_1' + H_{20}'$.

Dimensionless variables are formed in the following manner:

$$\left.\begin{aligned}
&(x, y) = (x', y')/L, \quad z = z'/H_0', \quad t = t' f_0, \\
&(u_i, v_i) = (u_i', v_i')/U, \quad w_i = w_i' L/(H_0' U), \\
&p_1 = [p_1' + \rho_1 g(z' - H_0')]/(\rho_1 U f_0 L), \\
&p_2 = [p_2' + \rho_2 g(z' - H_{20}') - \rho_1 g H_1']/(\rho_2 U f_0 L), \\
&h = h' g \Delta\rho/(\rho_2 U f_0 L), \quad f = (f_0 - \beta' y')/f_0 = 1 - \beta y, \\
&(H_1, H_2, H) = (H_1', H_2', H')/H_0',
\end{aligned}\right\} \tag{2.1}$$

where $i = 1, 2$ and where subscripts 1, 2 denote variables in the upper and lower layers, respectively. The variables $(u', v', w')$ are the velocity components in the $(x', y', z')$ directions, $p'$ is the pressure, $h'$ is the perturbation height of the density interface above $H_{20}'$, $t'$ is time, $L$ is a characteristic horizontal alongshore scale, $U$ is a characteristic horizontal velocity, $f_0$ is the value of the Coriolis parameter at a reference latitude, and $\beta = \beta' L/f_0$.

We assume that the motion in each layer is inviscid and linear. We also assume that $H_0'/L$, $H_0'/L_s \ll 1$ so that the motion is hydrostatic. The continuity and momentum equations are integrated over the depth in each layer to give the following set of equations (e.g. Allen 1975):

$$(H_1 u_1)_x + (H_1 v_1)_y = \tilde{S}^{-1} h_t, \tag{2.2a}$$

$$[u_{1t}] - f v_1 = -p_{1x}, \tag{2.2b}$$

$$v_{1t} + f u_1 = -p_{1y}, \tag{2.2c}$$

$$(H_2 u_2)_x + (H_2 v_2)_y = -\tilde{S}^{-1} h_t, \tag{2.3a}$$

$$[u_{2t}] - f v_2 = -p_{2x}, \tag{2.3b}$$

$$v_{2t} + f u_2 = -p_{2y}. \tag{2.3c}$$

Here subscripts $(x, y, t)$ denote partial differentiation,

$$h = p_2 - p_1, \tag{2.4}$$

$\tilde{S}$ is the stratification parameter at $f_0$,

$$\tilde{S} = (N H_0'/f_0 L)^2 \tag{2.5}$$

and $N^2 = g\Delta\rho/(\rho_2 H_0')$ is the square of the Brunt–Väisälä frequency. The square brackets in (2.2*b*) and (2.3*b*) denote terms that will be neglected under assumptions made below.

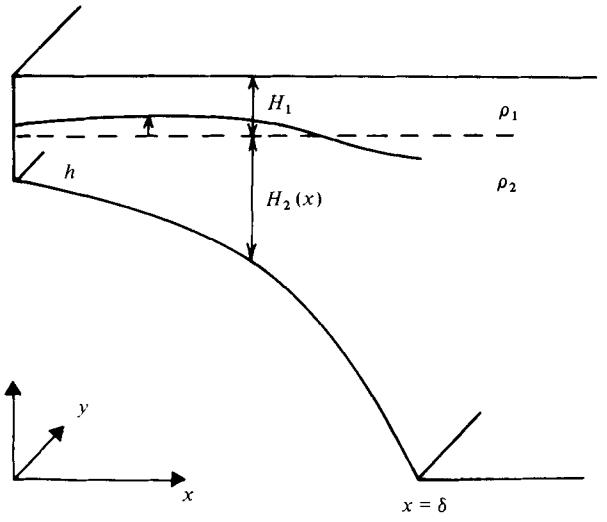


FIGURE 2. General configuration of the two-layer model for the continental shelf and slope region.

The coastline lies along $x = 0$ and the bottom topography is given by

$$H = H(x), \quad 0 \leqslant x \leqslant \delta, \tag{2.6a}$$

$$H = 1, \quad \delta \leqslant x, \tag{2.6b}$$

where $\delta = L_s/L$. It is assumed that the boundary at the coast is vertical, i.e.

$$H(x = 0) = H_{(0)} \neq 0,$$

and that the interface intersects the vertical section of the coast, i.e. $H_{(0)} > H_1$. The geometry is shown in figure 2.

We consider motions on a time scale $\delta_t$ which is large compared with an inertial period, i.e. where

$$\delta_t \gg 1. \tag{2.7}$$

If (2.2$a$) and (2.3$a$) are added, we see that a mass transport stream function may be defined, such that

$$\psi_y = u_1 + (H_2/H_1)\, u_2, \quad -\psi_x = v_1 + (H_2/H_1)\, v_2. \tag{2.8a,b}$$

In terms of $\psi$ and $h$, the velocity components are [with assumption (2.7)]

$$u_1 = H^{-1}[H_1\psi_y + f^{-2}H_2(fh_y + h_{xt})], \tag{2.9a}$$

$$u_2 = H^{-1}[H_1\psi_y - f^{-2}H_1(fh_y + h_{xt})], \tag{2.9b}$$

$$v_1 = H^{-1}[-H_1\psi_x - f^{-2}H_2(fh_x - [h_{yt}])], \tag{2.9c}$$

$$v_2 = H^{-1}[-H_1\psi_x + f^{-2}H_1(fh_x - [h_{yt}])]. \tag{2.9d}$$

Next we combine (2.2) and (2.3) into two governing equations for the variables $\psi$ and $h$ by deriving vorticity equations for the mass transport and for the velocity differences (Allen 1975):

$$(\psi_{xx} + \psi_{yy} - \tilde{\delta}_B^{-1}\psi_x)_t + \tilde{\delta}_B^{-1}(f\psi_y - h_y) + f_y\psi_x = 0, \tag{2.10a}$$

$$(h_{xx} + h_{yy} + a\tilde{\delta}_B^{-1}h_x - f^2\tilde{\delta}_R^{-2}h)_t - a\tilde{\delta}_B^{-1}f(f\psi_y - h_y) + f_y h_x = 0, \tag{2.10b}$$

where $\tilde{\delta}_B^{-1} = H_x/H$, $a = H_1/H_2$, $\tilde{\delta}_R^2 = \tilde{S}\bar{H}$ and $\bar{H} = H_1 H_2/H$. The function

$$\tilde{\delta}_R/f = \tilde{\delta}_R(x)/f(y)$$

is the local internal Rossby radius of deformation.

We assume that the width of the shelf–slope region is small compared with scales typical of alongshore variations in the flow field, i.e.

$$\delta \ll 1. \tag{2.11}$$

To describe the motion on the shelf it is useful to define a new cross-shelf variable

$$\xi = x/\delta, \tag{2.12a}$$

where $H_\xi/H = \delta H_x/H = O(1)$. The equations (2.10$a, b$) then imply that a natural time scale is

$$\bar{t} = t\delta. \tag{2.12b}$$

In terms of $\xi$ and $\bar{t}$, the approximate governing equations for the shelf and slope region with (2.11) are

$$(\psi_{\xi\xi} - \delta_B^{-1}\psi_\xi)_{\bar{t}} + \delta_B^{-1}(f\psi_y - h_y) + f_y\psi_\xi = 0, \tag{2.13a}$$

$$(h_{\xi\xi} + a\delta_B^{-1}h_\xi - (f/\delta_R)^2 h)_{\bar{t}} - a\delta_B^{-1}f(f\psi_y - h_y) + f_y h_\xi = 0, \tag{2.13b}$$

where

$$\delta_R = \tilde{\delta}_R/\delta = (S\bar{H})^{\frac{1}{2}}, \quad S = \tilde{S}/\delta^2, \quad \delta_B = \tilde{\delta}_B/\delta = H_\xi/H. \tag{2.13c, d, e}$$

(The shelf–slope width $L_s$ is used in the non-dimensionalization of $\delta_R$, $S$ and $\delta_B$, whereas the alongshore scale $L$ is used for $\tilde{\delta}_R$, $\tilde{S}$ and $\tilde{\delta}_B$.)

Assumption (2.11) is the standard long-wave approximation for coastal trapped waves (e.g. Gill & Schumann 1974). With the scalings (2.12$a, b$), the alongshore velocity components on the shelf ($v_1$, $v_2$) are $O(\delta^{-1})$ and the terms in square brackets in (2.2$b$), (2.3$b$) and the $h_{yt}$ term in (2.9$c, d$) may be neglected. As a result, the alongshore component of velocity is assumed to be in geostrophic balance. The major simplifying result of (2.11) is to make all of the coastal trapped waves in the present problem non-dispersive.

The internal Rossby radius of deformation, evaluated at the interior depth $\tilde{\delta}_I(x = 1)/f = \tilde{\delta}_{R(1)}/f$, gives the interior offshore decay scale for baroclinic disturbances. We will assume that this scale is also small compared with the alongshore scale, i.e.

$$\tilde{\delta}_{R(1)}/f \ll 1. \tag{2.14}$$

In the interior, $\tilde{\delta}_B^{-1} = 0$ and $\tilde{\delta}_R = \tilde{\delta}_{R(1)}$. With the interior variables denoted by a subscript $I$, the approximate governing equations are

$$(\psi_{Ixx} + \psi_{Iyy})_{\bar{t}} + \delta^{-1}f_y\psi_{Ix} = 0, \tag{2.15a}$$

$$(h_{Ixx} - (f/\tilde{\delta}_{R(1)})^2 h_I)_{\bar{t}} + \delta^{-1}f_y h_{Ix} = 0, \tag{2.15b}$$

where (2.14) has been used to neglect $h_{yy}$ in (2.15$b$).

The boundary conditions at the coast for (2.13$a, b$) are

$$\psi_y = 0, \quad h_{\xi\bar{t}} + fh_y = 0 \quad \text{at} \quad \xi = 0. \tag{2.16a}$$

The boundary conditions for (2.15$a, b$), appropriate for coastal trapped waves, are

$$\psi_{Ix}, \psi_{Iy} \to 0, \quad h_{Ix}, h_{Iy} \to 0 \quad \text{as} \quad x \to \infty. \tag{2.16b}$$

The matching conditions for the interior and shelf solutions at $x = \delta$ follow from the requirement for continuity of the normal velocity components and of the pressure. These conditions are

$$\psi_y = \psi_{Iy}, \quad \psi_x = \psi_{Ix}, \quad h = h_I, \quad h_x = h_{Ix} \quad \text{at} \quad x = \delta. \tag{2.16c}$$

The variation of the Coriolis parameter with $y$ is treated here by assuming that the alongshore scale of variation of the waves is small compared with the $y$ scale of variation of the Coriolis parameter, i.e. that $|f(df/dy)^{-1}| \gg 1$, which is equivalent to

$$\beta/f \ll 1. \tag{2.17}$$

As a result, $f$ varies slowly on the alongshore scale of the waves and the problem reduces to that for the propagation of waves in a slowly varying environment. The assumption (2.17) leads naturally to the definition of the slow variable

$$Y = \beta y, \tag{2.18}$$

such that $f = f(Y) = 1 - Y$.

To summarize the assumptions made concerning the spatial scales, the onshore–offshore scales $\delta$ and $\tilde{\delta}_{R(1)}/f$ are assumed in (2.11) and (2.14) to be small compared with the $O(1)$ alongshore scale characteristic of the wave motion. The latter, in turn, is assumed in (2.17) to be small compared with the $y$ scale of variation of the Coriolis parameter. All of these are reasonable for a large class of coastal trapped waves.

## 3. Solutions for constant $f$

We first consider the nature of the coastal trapped waves described by (2.13), (2.15) and (2.16) for a constant $f$, i.e. with $f_y = 0$. We look for free-wave solutions in the form

$$[\psi, h] = [\phi(\xi), g(\xi)]\,\mathrm{Re}\{A \exp[-i\omega(\bar{t} + c^{-1}y)]\}, \tag{3.1a,b}$$

where $\omega$ is the radian frequency, $c$ is the phase velocity in the negative $y$ direction, $A$ is a complex constant with $|A| = 1$, and Re denotes the real part.

Substituting (3.1$a$, $b$) in (2.13$a$, $b$) and in (2.16$a$), we obtain

$$(\phi_{\xi\xi} - \delta_B^{-1}\phi_\xi) + (\delta_B c)^{-1}(f\phi - g) = 0, \tag{3.2a}$$

$$(g_{\xi\xi} + a\delta_B^{-1}g_\xi - (f/\delta_R)^2 g) - a(\delta_B c)^{-1} f(f\phi - g) = 0, \tag{3.2b}$$

$$\phi = 0, \quad g_\xi + (f/c)g = 0 \quad \text{at} \quad \xi = 0. \tag{3.3a,b}$$

A boundary condition for the shelf variables at $\xi = 1$ may be derived by substituting

$$[\psi_I, h_I] = [\phi_I(x), g_I(x)]\,\mathrm{Re}\{A \exp[-i\omega(\bar{t} + c^{-1}y)]\}. \tag{3.4a,b}$$

in the interior equations (2.15), solving for $\phi_I$ and $g_I$ with boundary conditions (2.16$b$), applying the matching conditions (2.16$c$), and utilizing (2.11). The result is

$$\phi_\xi = 0, \quad g_\xi + (f/\delta_{R(1)})g = 0 \quad \text{at} \quad \xi = 1. \tag{3.5a,b}$$

The solutions to (3.2), (3.3) and (3.5) are eigenfunctions $(\phi_n, g_n)$ with corresponding

eigenvalues $c_n$. An orthogonality relation for the eigenfunctions is most conveniently derived if (3.2$a, b$) are rewritten in the form

$$(\phi_\xi/H)_\xi + (H_\xi/H^2)\, c^{-1}(f\phi - g) = 0, \tag{3.6a}$$

$$(g_\xi/aH)_\xi - f^2(SH_1^2)^{-1} g - f(H_\xi/H^2)\, c^{-1}(f\phi - g) = 0. \tag{3.6b}$$

By multiplying (3.6$a$) and (3.6$b$) for ($\phi_n, g_n$) by, respectively, $\phi_m$ and $g_m$, doing this again with the $n$ and $m$ reversed, integrating the four equations over $\xi$ from 0 to 1 and combining, we obtain the orthogonality relation

$$\frac{1}{2}\left\{\int_0^1 [H^{-1}(\phi_{n\xi}\phi_{m\xi} + (af^2)^{-1} g_{n\xi} g_{m\xi}) + (SH_1^2)^{-1} g_n g_m]\, d\xi + (f\delta_{R(1)} a_{(1)} H_{(1)})^{-1} g_n(1)\, g_m(1)\right\} = \delta_{nm}\, \mathscr{E}_n, \tag{3.7}$$

where $\delta_{mn}$ is the Kronecker delta and where $\mathscr{E}_n$ is the average energy density in each mode:

$$\mathscr{E}_n = \frac{1}{2}\left\{\int_0^1 [H^{-1}(\phi_{n\xi}^2 + (af^2)^{-1} g_{n\xi}^2) + (SH_1^2)^{-1} g_n^2]\, d\xi + (f\delta_{R(1)} a_{(1)} H_{(1)})^{-1} g_n^2(1)\right\}. \tag{3.8}$$

By combining the integrated equations in a different manner we may obtain an alternative orthogonality relation:

$$\tfrac{1}{2} f^{-1}\left[\int_0^1 (H_\xi/H^2)\,(f\phi_n - g_n)\,(f\phi_m - g_m)\, d\xi + (a_{(0)} H_{(0)})^{-1} g_n(0)\, g_m(0)\right] = \delta_{nm} c_n\, \mathscr{E}_n, \tag{3.9}$$

where, with (3.8), the factor on the right-hand side of (3.9) follows from multiplying (3.6$a, b$) for ($\phi_n, g_n$) by, respectively, $\phi_n$ and $g_n$, integrating over $\xi$ from 0 to 1 and combining. The result is

$$c_n\, \mathscr{E}_n = \tfrac{1}{2} f^{-1}\left[\int_0^1 (H_\xi/H^2)\,(f\phi_n - g_n)^2\, d\xi + (a_{(0)} H_{(0)})^{-1} g_n^2(0)\right]. \tag{3.10}$$

To illustrate the nature of the solutions to (3.2), (3.3) and (3.5), it is desirable to obtain analytical results. This is difficult in general because of the variable coefficients in (3.2$a, b$). If the exponential shelf profile of Buchwald & Adams (1968) is used, $\delta_B$ is a constant and constant coefficients arise in (3.2$a$). Variable coefficients remain, however, in (3.2$b$) and analytical solutions are still elusive. That case was solved by Allen (1975) with perturbation methods for $\delta_{R(0)} \ll 1$. It is also possible to obtain perturbation solutions to (3.2$a, b$) for general values of $\delta_R$ if it is assumed that $a = H_1/H_2 \ll 1$. That procedure is outlined in appendix A for the exponential slope. In the present problem, the essential qualitative features of the solutions may be clearly illustrated with a very idealized 'weak slope' model for which analytical results are easily obtained for general $\delta_R$. In this model, shown in figure 3, the continental shelf–slope region is represented by a linear bottom slope of small magnitude, i.e. by $H = 1 + \delta_B^{-1}(\xi - 1)$, where $\delta_B$ is a constant and $\delta_B^{-1} \ll 1$. This is, of course, the large-$\delta_B$ limit of the exponential slope.

With the 'weak slope' model, (3.2$a, b$) simplify to

$$\phi_{\xi\xi} + (\delta_B c)^{-1}(f\phi - g) = 0, \tag{3.11a}$$

$$(g_{\xi\xi} - (f/\delta_R)^2 g) - a(\delta_B c)^{-1} f(f\phi - g) = 0, \tag{3.11b}$$

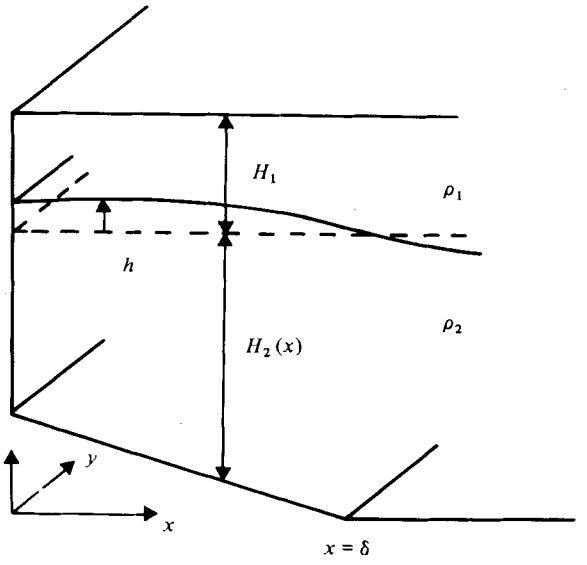


FIGURE 3. The geometry of the 'weak slope' model.

where $\delta_B$, $\delta_R = \delta_{R(1)}$, and $a = H_1/H_{2(1)}$ are constants. An implicit assumption involved in the formation of (3.11*b*) is that $\delta_B \gg a(\delta_R/f)$. For future use, we define

$$\gamma^2 = f(\delta_B c)^{-1}. \tag{3.11c}$$

The boundary conditions are given by (3.3) and (3.5).

Since all the coefficients in (3.11*a*, *b*) are constant, explicit analytical solutions may be determined readily. The algebra simplifies even further and the physical structure of the results becomes more transparent, however, if (3.11*a*, *b*) are solved by perturbation methods assuming that

$$a \ll 1. \tag{3.12}$$

Using assumption (3.12), approximate solutions may be obtained in the following manner. With the variables expanded as

$$\phi = \hat{\phi}_n + \ldots, \quad g = a\hat{g}_n + \ldots, \quad c = c_n + \ldots, \tag{3.13a,b,c}$$

the lowest-order approximations to (3.11*a*, *b*) are

$$\hat{\phi}_{n\xi\xi} + (\delta_B c_n)^{-1} f \hat{\phi}_n = 0, \tag{3.14a}$$

$$\hat{g}_{n\xi\xi} - (f/\delta_R)^2 \hat{g}_n = (\delta_B c_n)^{-1} f^2 \hat{\phi}_n. \tag{3.14b}$$

Equation (3.14*a*) is uncoupled from (3.14*b*) and may be solved directly for $\hat{\phi}_n$. The solutions are

$$\hat{\phi}_n = D_n \sin k_n \xi, \quad k_n = \tfrac{1}{2}(2n-1)\pi, \quad n = 1, 2, \ldots, \tag{3.15a}$$

$$\hat{g}_n = D_n k_n^2 f (k_n^2 + (f/\delta_R)^2)^{-1} [-\sin k_n \xi + E_n \exp(-\xi f/\delta_R) + F_n \exp(-f(1+\xi)/\delta_R) + G_n \exp(-f(1-\xi)/\delta_R)], \tag{3.15b}$$

where

$$E_n = -k_n c_n \delta_R f^{-1}(c_n - \delta_R)^{-1}, \tag{3.15c}$$

$$F_n = \tfrac{1}{2}\sin k_n (c_n + \delta_R)(c_n - \delta_R)^{-1}, \tag{3.15d}$$

$$G_n = \tfrac{1}{2}\sin k_n = \tfrac{1}{2}(-1)^{n-1}. \tag{3.15e}$$

The wave speed is given by

$$c_n = f(\delta_B k_n^2)^{-1}. \tag{3.16}$$

One additional solution exists and may be found using the scaling

$$g = \tilde{g}_0 + \ldots, \quad \phi = \tilde{\phi}_0 + \ldots, \quad c = c_0 + \ldots. \tag{3.17a,b,c}$$

With (3.17$a,b,c$), (3.11$a,b$) become

$$\tilde{g}_{0\xi\xi} - (f/\delta_R)^2 \tilde{g}_0 = 0, \tag{3.18a}$$

$$\tilde{\phi}_{0\xi\xi} + (\delta_B c_0)^{-1} f \tilde{\phi}_0 = (\delta_B c_0)^{-1} \tilde{g}_0. \tag{3.18b}$$

In this case, (3.18$a$) may be solved directly for $\tilde{g}_0$. The solution is

$$\tilde{g}_0 = C_0 \exp[-(f/\delta_R)\xi], \tag{3.19a}$$

$$\tilde{\phi}_0 = C_0[(f^2\delta_B)\delta_R^{-1} + f]^{-1}\{\exp[-(f/\delta_R)\xi] - \cos\gamma\xi + I\sin\gamma\xi\}, \tag{3.19b}$$

where

$$I = [f(\gamma\delta_R)^{-1}\exp(-f/\delta_R) - \sin\gamma]/\cos\gamma, \tag{3.19c}$$

and where $\gamma$ is given by (3.11$c$) with (3.17$c$). The wave speed is determined by (3.3$b$) and is

$$c_0 = \delta_R. \tag{3.20}$$

Consequently, for values of the parameters where the above procedure is valid, the eigenfunctions $(\phi_n, g_n)$ $[n = 0, 1, 2, \ldots]$ are comprised of the set of solutions $(\hat{\phi}_n, \hat{g}_n)$ $[n = 1, 2, \ldots]$ and the single solution pair $(\tilde{\phi}_0, \tilde{g}_0)$. The solutions $\hat{\phi}_n$ have a cross-shelf structure similar to barotropic continental-shelf waves (e.g. Buchwald & Adams 1968). We will refer to $(\hat{\phi}_n, \hat{g}_n)$ as the shelf-wave solutions. The vertical structure of the velocity field given by these solutions, however, depends on $\delta_R$. For $\delta_R \ll 1$, the velocity field is approximately depth independent and these are essentially the barotropic continental-shelf waves that would exist if the stratification were absent. For $\delta_R \gg 1$, $\hat{g}_n \sim -f\hat{\phi}_n$, which implies $u_1, v_1 \sim 0$, and the waves are 'bottom trapped', i.e. the motion is confined to the bottom layer (Rhines 1970). We will refer to the single solution pair $(\tilde{\phi}_0, \tilde{g}_0)$ as the internal Kelvin wave. The structure of $\tilde{g}_0$ and the wave speed (3.20) are identical to those found for a flat-bottom internal Kelvin wave. In this case, however, there is a barotropic contribution to the onshore velocities from $\tilde{\phi}_0$, so that $u_1, u_2 \neq 0$. For all of the eigenfunctions the phase velocity is positive $c > 0$, so that the propagation is poleward.

We use the term eigenfunction specifically to represent a single solution pair $(\phi_n, g_n)$ whose eigenvalue $c_n$ has a continuous dependence on the parameters of the problem, for example on $f$. We use the term wave more loosely to represent one of the solutions with certain physical characteristics, for example shelf wave for $(\hat{\phi}_n, \hat{g}_n)$ or internal Kelvin wave for $(\tilde{\phi}_0, \tilde{g}_0)$.

Note that $\hat{g}_n$ is unbounded (3.15$c,d$) if $c_n = \delta_R$ and that $\tilde{\phi}_0$ is unbounded (3.19$c$) if

$\gamma^2 = f(\delta_B \delta_R)^{-1} = k_n^2$, so that $\cos\gamma = 0$. This is the case if the wave speed obtained in (3.20) for the internal Kelvin wave coincides with the indicated wave speed (3.16) of one of the shelf-wave solutions, which occurs when

$$\delta_R = f(\delta_B k_n^2)^{-1}. \tag{3.21}$$

Near these values of the parameters, the method used in finding the solutions (3.15) and (3.19) is invalid and a different procedure must be followed. In the 'weak slope' geometry, with $\delta_B \gg 1$ and $f = O(1)$, the equality (3.21) can only occur when $\delta_R \ll 1$ and hence when the self-wave solutions are barotropic.

Next we examine the solutions when the parameter values are in the vicinity of points like (3.21). The two types of solutions, (3.15) and (3.19), must be considered simultaneously in these regions. It is assumed, consistent with (3.21), that $\delta_R \ll 1$. In this limit, no assumption about the magnitude of $a$ is necessary.

In a manner similar to that used before for $a \ll 1$, approximate solutions for $\delta_R \ll 1$ may be written

$$\phi = D\sin\gamma\xi + C\delta_R^2(c\delta_B f^2)^{-1}[\exp(-f\xi/\delta_R) - \cos\gamma\xi], \tag{3.22a}$$

$$g = C\exp(-f\xi/\delta_R) - D\delta_R^2 a(\delta_B c)^{-1}\sin\gamma\xi + E\exp(f(\xi-1)/\delta_R), \tag{3.22b}$$

where

$$E = \tfrac{1}{2}D[\delta_R^2 a(\delta_B c)^{-1}][\delta_R \gamma f^{-1}\cos\gamma + \sin\gamma], \tag{3.22c}$$

and where (3.22$a, b$) satisfy the boundary conditions (3.3$a$) and (3.5$b$).

Substituting (3.22$a, b$) in the two additional boundary conditions (3.3$b$) and (3.5$a$), we obtain

$$C(\delta_R^{-1} - c^{-1}) + D\gamma\delta_R^2 a(\delta_B cf)^{-1} = 0, \tag{3.23a}$$

$$C\delta_R^2(\delta_B cf^2)^{-1}\sin\gamma + D\cos\gamma = 0, \tag{3.23b}$$

where we have neglected the exponentially small term $E\exp(-f/\delta_R)$ in (3.23$a$). The requirement that (3.23$a, b$) be compatible gives an equation for the eigenvalue $c$:

$$\cos\gamma(\delta_R^{-1} - c^{-1}) = R, \tag{3.24a}$$

where

$$R = a\delta_R^4 \gamma f^{-3}(\delta_B c)^{-2}\sin\gamma. \tag{3.24b}$$

The term $R$ on the right-hand side of (3.24$a$) is small and may be neglected if either of the two factors in the term on the left-hand side are greater in magnitude than $R$. Under these conditions, the approximate solutions to (3.24) are the following.

For $|\delta_R^{-1} - c^{-1}| \gg |R|$:

$$\left.\begin{aligned} &\cos\gamma = 0, \quad \gamma = k_n, \quad c_n = f(\delta_B k_n^2)^{-1}, \\ &D_n = O(1), \quad C_n = O(\delta_R^3)\, D_n. \end{aligned}\right\} \tag{3.25}$$

These are the shelf-wave solutions (3.15).

For $|\cos\gamma| \gg |R|$:

$$c_0 = \delta_R, \quad C_0 = O(1), \quad D_0 = O(\delta_R/\delta_B)C_0. \tag{3.26}$$

This is the internal-Kelvin-wave solution (3.19).

When $\delta_R \simeq f(\delta_B k_n^2)^{-1}$, both factors in the term on the left-hand side of (3.24$a$) are small and $R$ must be retained to obtain the solution. We assume that this condition is approached through the variation of the Coriolis parameter $f$. Consider the value of

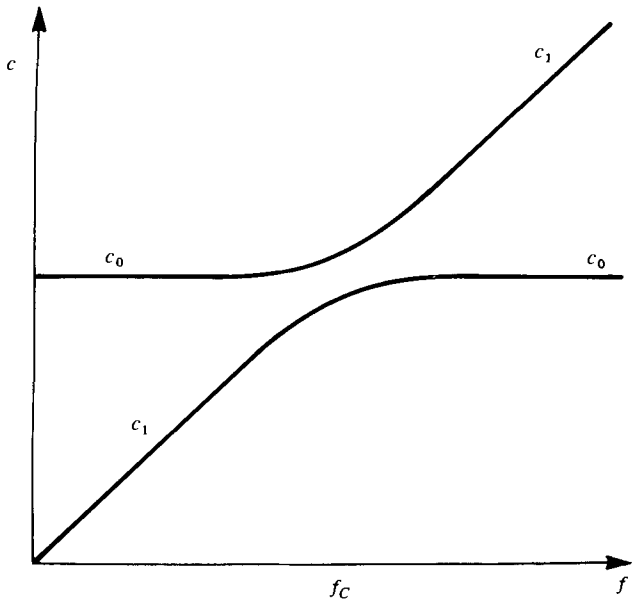


FIGURE 4. Schematic of the variation of the wave speeds as a function of $f$ for the two eigenfunctions which, for $f < f_C$, represent the internal Kelvin wave and the $n = 1$ shelf wave.

$f$ to be initially small enough that $c_n < \delta_R$ for all $n$. As the magnitude of $f$ increases, a critical value

$$f_C = \delta_R \delta_B k_1^2 \tag{3.27}$$

is reached where the wave speeds of the internal Kelvin wave and the first ($n = 1$) shelf-wave solution, as given by (3.25) and (3.26), are equal.

A solution for $c$ is sought in the neighbourhood of $f = f_C$. We expand about that point by letting

$$f = f_C(1+\tilde{f}), \quad c = c_C(1+\tilde{c}), \tag{3.28a,b}$$

where $c_C = \delta_R$, and $\tilde{f}, \tilde{c} \ll 1$. The approximate solution obtained from (3.24) is

$$\tilde{c}_\pm = \tfrac{1}{2}[\tilde{f} \pm (\tilde{f}^2 + K)^{\frac{1}{2}}], \tag{3.29a}$$

where

$$K = 8a\delta_R^3(\delta_B^2 f_C^3)^{-1}. \tag{3.29b}$$

For $\tilde{f} = 0$,

$$\tilde{c}_\pm = \tilde{c}_{C\pm} = \pm \tfrac{1}{2}K^{\frac{1}{2}} = \pm (2a\delta_R^3)^{\frac{1}{2}}(\delta_B f_C^{\frac{3}{2}})^{-1}, \tag{3.30a}$$

$$D = \mp (2\delta_B/a)^{\frac{1}{2}} f_C^{-1} C. \tag{3.30b}$$

For $\tilde{f} > 0$ and $\tilde{f}^2 \gg K$,

$$\tilde{c}_+ \sim \tilde{f}, \quad C \sim -\delta_R^3 \tilde{f}^{-1} D, \tag{3.31a,b}$$

$$\tilde{c}_- \sim 0, \quad D \sim (\delta_R/\delta_B)\tilde{f}^{-1} C. \tag{3.31c,d}$$

For $\tilde{f} < 0$ and $\tilde{f}^2 \gg K$,

$$\tilde{c}_+ \sim 0, \quad D \sim (\delta_R/\delta_B)\tilde{f}^{-1} C, \tag{3.32a,b}$$

$$\tilde{c}_- \sim \tilde{f}, \quad C \sim -\delta_R^3 \tilde{f}^{-1} D. \tag{3.32c,d}$$

A plot of the wave speeds for these two eigenfunctions as a function of $f$ is given in figure 4. We can see from this plot and from (3.31) and (3.32) that the eigenfunction

which represents an internal Kelvin wave for $f < f_C$ changes structure and wave speed as $f$ increases so that for $f > f_C$ it represents the $n = 1$ continental-shelf wave. When $f = f_C$, the eigenfunction is composed of a combination (3.30*b*) of both type waves and has a wave speed $c_C(1+\tilde{c}_{C_+})$. The eigenfunction which is the $n = 1$ shelf wave for $f < f_C$ transforms as $f$ is increased so that for $f > f_C$ it becomes an internal Kelvin wave. The variation with $f$ of the cross-shelf structure of the velocity components associated with these two eigenfunctions is shown, for the exponential slope solutions, in figures 5 and 6 of appendix A. The fact that the eigenfunctions change structure to represent a different type of wave as $f$ varies plays a central role in the following sections.

## 4. Solutions for slowly varying $f$

We now consider the coastal trapped-wave solutions to (2.13), (2.15) and (2.16) when $f$ is a slowly varying function of $y$. In this case, $f = f(Y)$, $Y = \beta y$, and $\beta \ll 1$. Free wave solutions are sought in the form

$$[\psi, h, \psi_I, h_I] = \mathrm{Re}\left\{[\phi, g, \phi_I, g_I]\exp\left[-i\omega\left(\bar{t}+\int_{y_0}^{y} c^{-1}\,dy\right)\right]\right\}, \tag{4.1}$$

where here $c = c(Y)$ and the variables $\phi$, $g$, $\phi_I$, $g_I$ also depend parametrically on $Y$, for example $\phi = \phi(\xi;\ Y)$.

The solutions for the interior variables, which satisfy boundary condition (2.16*b*) are

$$\phi_I = B\exp[p_1(x-\delta)], \quad g_I = C\exp[p_2(x-\delta)], \tag{4.2a,b}$$

where, with (2.11),

$$p_1 \simeq -\delta^{-1}[i(\tfrac{1}{2}\beta f_Y/\omega)+\delta|\omega/c|], \tag{4.2c}$$

$$p_2 \simeq -\delta^{-1}[i(\tfrac{1}{2}\beta f_Y/\omega)+(f/\delta_{R(1)})], \tag{4.2d}$$

and where the following assumptions, consistent for coastal trapped waves with $\beta \ll 1$, have been made (see §5):

$$(\tfrac{1}{2}\beta f_Y/\omega)^2 \ll (\delta\omega/c)^2,\ (f/\delta_{R(1)})^2. \tag{4.2e,f}$$

Boundary conditions for the shelf variables at $\xi = 1$ may be derived by using the interior solutions (4.2) and the matching conditions (2.16*c*). These are

$$\phi_\xi = (-\tfrac{1}{2}i\beta f_Y\omega^{-1}-\delta|\omega/c|)\phi \quad \text{at} \quad \xi = 1, \tag{4.3a}$$

$$g_\xi+(f/\delta_{R(1)})g = -i(\tfrac{1}{2}\beta f_Y/\omega)g \quad \text{at} \quad \xi = 1. \tag{4.3b}$$

The equations for the shelf variables are

$$(\phi_\xi/H)_\xi+(H_\xi/H^2)c^{-1}(f\phi-g) = i\beta\,\mathrm{RHS}_1, \tag{4.4a}$$

$$(g_\xi/aH)_\xi-f^2(SH_1^2)^{-1}g-f(H_\xi/H^2)c^{-1}(f\phi-g) = i\beta\,\mathrm{RHS}_2, \tag{4.4b}$$

where

$$\mathrm{RHS}_1(\phi,g) = -\omega^{-1}[f_Y H^{-1}\phi_\xi+(H_\xi/H^2)(f\phi_Y-g_Y)], \tag{4.4c}$$

$$\mathrm{RHS}_2(\phi,g) = -\omega^{-1}[f_Y(aH)^{-1}g_\xi-f(H_\xi/H^2)(f\phi_Y-g_Y)]. \tag{4.4d}$$

The boundary conditions at $\xi = 0$ are

$$\phi = -i\beta(c/\omega)\phi_Y, \quad g_\xi+(f/c)g = -i\beta(f/\omega)g_Y \quad \text{at} \quad \xi = 0. \tag{4.5a,b}$$

The solutions are expanded in the form

$$\phi = A(\phi_0 + i\beta\phi_1 + \ldots), \quad g = A(g_0 + i\beta g_1 + \ldots), \tag{4.6a,b}$$

where $A$ is a complex constant with $|A| = 1$, $\phi_0$, $\phi_1$, $g_0$, $g_1$ are real variables, and the subscript $n$ denoting the eigenfunction, for example $\phi = \phi_n$, $\phi_0 = \phi_{0n}$, has been dropped. Substituting (4.6$a,b$) into (4.3), (4.4) and (4.5), we find that the lowest-order solutions $\phi_0$ and $g_0$ satisfy the same equations and boundary conditions as the constant $f$ solutions (3.6), (3.3) and (3.5), but with $f = f(Y)$.

The equations for $\phi_1$ and $g_1$ are

$$(\phi_{1\xi}/H)_\xi + (H_\xi/H^2)\, c^{-1}(f\phi_1 - g_1) = \mathrm{RHS}_1(\phi_0, g_0), \tag{4.7a}$$

$$(g_{1\xi}/aH)_\xi - f^2(SH_1^2)^{-1} g_1 - f(H_\xi/H^2)\, c^{-1}(f\phi_1 - g_1) = \mathrm{RHS}_2(\phi_0, g_0), \tag{4.7b}$$

with boundary conditions

$$\phi_1 = 0, \quad g_{1\xi} + (f/c)\, g_1 = -(f/\omega)\, g_{0Y} \quad \text{at} \quad \xi = 0, \tag{4.8a,b}$$

$$\phi_{1\xi} = -(\tfrac{1}{2} f_Y/\omega)\, \phi_0, \quad g_{1\xi} + (f/\delta_{R(1)})\, g_1 = -(\tfrac{1}{2} f_Y/\omega)\, g_0 \quad \text{at} \quad \xi = 1. \tag{4.9a,b}$$

The second term on the right-hand side of (4.3$a$) indicates that an $O(\delta)$ real correction to $\phi_0$ is required. This $O(\delta\omega/c)$ term is, by assumption (4.2$e$), formally larger in magnitude than the $O(i\beta f_Y/\omega)$ term that appears in (4.9$a$). It is not necessary, however, for the determination of the $Y$ variation of the lowest-order solutions $\phi_0$, $g_0$ to consider the small $O(\delta)$ real corrections to $\phi_0$, $g_0$ and $c$ and they are neglected.

A compatibility condition for $\phi_1$ and $g_1$ (Ince 1956) may be determined by multiplying the equations (3.6$a,b$) and (4.7$a,b$) in the following manner: (3.6$a$) and (3.6$b$) for $(\phi_0, g_0)$ by, respectively, $\phi_1$ and $g_1$; (4.7$a$) by $\phi_0$ and (4.7$b$) by $g_0$. These four equations are then integrated over $\xi$ from 0 to 1. Utilizing the boundary conditions (3.3), (3.5), (4.8), (4.9) and combining the results, we obtain

$$\frac{d}{dY}\left[f^{-1}\int_0^1 (H_\xi/H^2)\,(f\phi_0 - g_0)^2\, d\xi + (f a_{(0)} H_{(0)})^{-1} g_0^2(0)\right] = 0, \tag{4.10a}$$

which, with (3.10), may be written as

$$(c_{0n}\mathscr{E}_{0n})_Y = 0. \tag{4.10b}$$

Equation (4.10) is simply an expression of the conservation of wave action, which reduces here to the statement that the flux of wave energy density $c_{0n}\mathscr{E}_{0n}$ along the coast is independent of $Y$ for each eigenfunction. This is a standard result for slowly varying waveguides (Bretherton 1968; for example for shelf waves, see Grimshaw 1977). It is implied by (4.10) that, as $Y$ varies, energy in a given eigenfunction will stay in that eigenfunction as long as the slowly varying approximation is valid. Evidently, this will be the case even if the structure of the eigenfunction changes from one type of wave to another, as was found in § 3 for values of $f$ around $f_C$. A simple mechanical system with an analogous type of behaviour is discussed briefly in appendix C.

For $f(Y)$ in the neighbourhood of $f_C$, or in the neighbourhood of other critical values of $f$ that satisfy (3.21), the coefficients $C_n$ and $D_n$ vary more rapidly with $Y$ than they do otherwise. It is desirable to examine the variation of the solutions in these regions to determine the requirement on the magnitude of $c/\omega$, in terms of the other parameters of the problem, such that the slowly varying approximation remains valid.

For the 'weak slope' model in § 3, $c_{0n}\mathscr{E}_{0n}$ reduces to

$$c_{0n}\mathscr{E}_{0n} = f^{-1}\int_0^1 \delta_B^{-1}(f\phi_{0n} - g_{0n})^2\,d\xi + (fa)^{-1}g_{0n}^2(0), \tag{4.11}$$

where $a$ and $\delta_B$ are constants. We assume that $\delta_R \ll 1$, consistent with (3.21). The solutions are given by (3.22$a, b$). Substituting (3.22$a, b$) in (4.11) and retaining only the largest terms, we find

$$c_{0n}\mathscr{E}_{0n} = \tfrac{1}{2}\delta_B^{-1}fD_n^2 + (fa)^{-1}C_n^2, \tag{4.12}$$

where we have made the approximation $\sin 2\gamma \simeq 0$ in the first term on the right-hand side of (4.12) based on the fact that, when $D_n^2$ is appreciable compared to $C_n^2$, $\gamma \simeq k_n$.

At $f = f_C$, the relation between $C_n$ and $D_n$ is given by (3.30$b$), which implies that the two terms on the right-hand side of (4.12) are equal in magnitude. Consequently, at $f_C$ the energy flux in a given eigenfunction is equally divided between the two types of waves.

To determine a requirement on $c/\omega$ for the validity of the slowly varying approximation, we examine the magnitude at $f_C$ of the ratio of a typical term on the right-hand side of (4.4$a, b$) and (4.5$a, b$) to an appropriate term on the left-hand side. An appropriate term on the left-hand side is one of the smallest terms which must be retained to obtain the lowest-order approximation for the eigenvalue $c$. For example, at $f = f_C$ (4.5$b$) is approximately

$$g_\xi + (f_C/c_C)(1-\tilde{c}_C)g = -i\beta(f_C/\omega)g_Y \quad \text{at} \quad \xi = 0 \tag{4.13}$$

and the ratio to be examined is

$$\beta(f_C/\omega)g_Y/[\tilde{c}_C(f/c_C)g] \simeq \beta(c_C/\omega)\tilde{c}_C^{-1}C_{nY}/C_n.$$

From (4.4$a$), we obtain in a similar manner the ratio

$$\beta(c_C/\omega)\tilde{c}_C^{-1}\phi_Y/\phi \simeq \beta(c_C/\omega)\tilde{c}_C^{-1}D_{nY}/D_n.$$

Utilizing (4.12) and (3.30$b$), we find that, at $f_C$, $D_{nY}/D_n = -C_{nY}/C_n$. Consequently, the magnitudes of these two terms at $f_C$ are similar and we concentrate on a determination of

$$R_1 = \beta(c_C/\omega)\tilde{c}_C^{-1}C_{nY}/C_n \quad \text{at} \quad f = f_C. \tag{4.14}$$

In the neighbourhood of $f_C$, (3.23$a$) is approximately

$$D_n \simeq -C_n\tilde{c}\delta_B f_C(a\delta_R^2 k_1)^{-1}. \tag{4.15}$$

Utilizing (4.12) and (4.15), we find

$$C_{nY}/C_n = \tfrac{1}{2}\tilde{c}_Y/\tilde{c} = \pm 1/(2f_C K^{\frac{1}{2}}) \quad \text{at} \quad f = f_C. \tag{4.16}$$

It follows from (4.16) and (3.29$a$) that

$$|R_1| = \beta|c_C/\omega|\,(f_C K)^{-1}. \tag{4.17}$$

We point out that, if a rough estimate of $R_1$ is made by approximating $C_{nY}/C_n$ around $f_C$ by $C_{nY}/C_n \simeq \Delta C_n(C_n\Delta Y)^{-1} \simeq (\Delta Y)^{-1} \simeq (f_C\Delta\tilde{f})^{-1}$ and, by estimating $\Delta\tilde{f} \simeq 2K^{\frac{1}{2}}$ from (3.29), an expression identical to (4.16) is obtained. For the validity of the slowly varying approximation it is necessary that $|R_1| \ll 1$, which implies

$$|c_C/\omega| \ll f_C K/\beta. \tag{4.18}$$

Note that, since $c_{1Y} = -c_1/f$ from (3.16), the parameter $R_1$ may be expressed as

$$R_1 = \beta|(c_C/\omega)c_{1YC}|\, c_C(\Delta c_C)^{-2}, \tag{4.19}$$

where $\Delta c_C = 2c_C|\tilde{c}_C|$ is the difference in wave speeds at $f_C$. It would therefore be possible to estimate the right-hand side of (4.18) graphically from an accurate plot of the eigenvalues $c$ versus $f$.

It is also possible to express $R_1$ as

$$R_1 = \beta l_{1YC}(\Delta l_C)^{-2}[1+O(\tilde{c}_C^2)], \tag{4.20}$$

where $l_1 = (\omega/c_1)$ is an alongshore wavenumber, $c_1$ is given by (3.16) and $\Delta l_C$ is the difference in wavenumber at $f_C$, i.e.

$$\Delta l_C = (\omega/c_C)[(1+\tilde{c}_{C+})^{-1} - (1+\tilde{c}_{C-})^{-1}]. \tag{4.21}$$

## 5. Discussion

The results from the analysis in § 3 and § 4 provide the answer, within the limits of the present idealized model, to the question posed in § 1 concerning the fate of wave energy which starts propagation poleward from the equatorial region in the form of a baroclinic internal Kelvin wave.

Equation (4.10) states that the flux of wave energy density in each eigenfunction is independent of $Y$. This implies, as long as the slowly-varying approximation remains valid, that energy present in one eigenfunction at low latitudes will remain in that eigenfunction as the wave propagates poleward. This will be the case even if the structure and wave speed of the eigenfunction change from one type of wave to another.

It was shown in § 3 that, for most values of $f$, the eigenfunctions are comprised of a set of shelf-wave solutions and an internal-Kelvin-wave solution. The wave speeds of the shelf waves vary linearly with $f$, whereas the wave speed of the internal Kelvin wave is independent of $f$. In the vicinity of critical values $f_C$ of $f$, where the wave speed of a shelf wave approaches that of the internal Kelvin wave, the eigenfunctions and eigenvalues vary. As shown in figure 4, the wave speeds, considered as a function of $f$, do not intersect, but veer off and exchange properties. Likewise, the eigenfunctions change so that they represent a different type of wave on either side of $f_C$. Consequently, the eigenfunction which has the structure and phase speed of an internal Kelvin wave at low latitudes ($f < f_C$) changes as $f$ increases through the critical value $f_C$ such that, for $f > f_C$, it has the structure and phase speed of the $n = 1$ shelf wave.

It follows from these results that an internal Kelvin wave which propagates poleward from the equatorial region where $f < f_C$ will transform into the $n = 1$ shelf wave, at values of $f$ near $f_C$, and will continue propagation poleward in that form.

To assess the implications for the wave motion off South America, estimates of numerical values of the parameters are required. For that purpose, we use the relations in appendix A derived from the exponential slope model under the assumption $a_{(0)} \ll 1$. Although that model is still highly idealized, the specific formulae derived from it should give more accurate approximations for parameter values under oceanic conditions than those from the 'weak slope' model. As shown in appendix A, the qualitative behaviour of the eigenfunctions in both cases is similar.

Details of the calculation of parameters are given in appendix B. Estimated values of the dimensional wave speed $c_1'$ of the $n = 1$ shelf-wave solution as a function of

latitude are listed in table 1. These values are obtained using the local shelf-slope width $L_s$. It may be seen that $c_1'$ generally increases as the latitude increases, reflecting the dependence on $f$, but that the variation is not monotonic owing to the variation of $L_s$. Using the estimate $c_0' = 100\,\mathrm{cm\,s^{-1}}$, we find that, as the latitude increases, $c_1' \simeq c_0'$ first at some point between 10° and 11° S.

We use the parameter values at the critical latitude near 10° to estimate in appendix B the magnitude of the restriction on the dimensional alongshore wavelength $\delta_y'$ so that the slowly-varying approximation is valid. This condition is obtained from (A 20), which is similar to (4.18), but with appropriate modifications from the exponential slope geometry. The result is

$$\delta_y' \ll L_V \simeq 1100\,\mathrm{km}. \tag{5.1}$$

Since the waves are non-dispersive, (5.1) may be converted, with $c_0' = 100\,\mathrm{cm\,s^{-1}}$, to a restriction on the period $T'$ of the fluctuations, which is $T' \ll 13$ days. Although some of the wave disturbances of interest may have wavelengths and periods that are too large to satisfy these conditions, the magnitude of $L_V$ does not appear to be so overly restrictive as to rule out the possible qualitative applicability of the results to a reasonably large class of coastal wave motions.† We note that the estimated $y'$ distance over which the transformation occurs is $L_V(2\pi)^{-1} \simeq 175\,\mathrm{km}$.

The assumption that the waves are coastally trapped (4.2$e$,$f$) also leads to restrictions on the period. For a given alongshore wavenumber ($\omega/c$), (4.2$e$,$f$) in dimensional variables are equivalent to $T' < T_1', T_2'$, where

$$T_1' = 2(2\pi)^2(\beta'\delta_y')^{-1} \quad \text{and} \quad T_2' = 2(2\pi)(\beta'\delta_R')^{-1}.$$

Since $\delta_y' \gg \delta_R'$ by (2.14), $T_1' \ll T_2'$. For $\delta_y' = 1100\,\mathrm{km}$, $T_1' = 36$ days, which leads to a less restrictive condition than that for slow variations.

The variability of $c_1'$ along the coast of South America indicates that the situation there is more complicated than represented in the present idealized model. The major qualitative difference results from the subsequent drop in magnitude of $c_1'$ below that of $c_0'$ in the region around 14° and 15° S. This variation occurs because the continental slope is very narrow in that location.

The effects of alongshore variations in topography were not included in the present model because the main point of interest concerned the effect of the monotonic latitudinal variation of $f$. The model could be extended to take into account slow alongshore variations in topography, as in Grimshaw (1977). A result similar to (4.10) would follow, and the shelf-wave solutions and wave speeds would be dependent on the local topography as well as on $f$. The conclusions would be similar to those stated here, since we have referred to local values of $c_1'$, but realistic alongshore variations in topography might lead to a more restrictive condition than (5.1).

The actual alongshore variations in slope topography off South America may result in substantial scattering of energy from one eigenfunction to another. In addition, it might be expected that scattering would be relatively large near critical latitudes where two eigenfunctions have similar wave speeds. Nevertheless, in spite of the possible complexity of the real situation, the qualitative behaviour found here would seem to

† It is likely, based on the analysis in Grimshaw & Allen (1979) for the linearly coupled, slowly varying oscillator problem, that the results will be approximately valid even if $\delta_y' \approx L_V$ (see Appendix C).

be of considerable interest. The primary result is that, for an internal Kelvin wave that satisfies (5.1) and propagates poleward over a continental margin, the *direct* route, i.e. the route that does not involve or depend on scattering, includes the transformation near a critical latitude to a shelf wave and the subsequent propagation poleward in that form.

Given that there is considerable observational evidence for the propagation of disturbances at mid-latitudes in the form of barotropic continental shelf waves, this result indicates that energy in baroclinic disturbances in the equatorial region may be able to propagate efficiently to higher latitudes where it may eventually take the form of barotropic shelf waves.

This research was supported by National Science Foundation grants DES75-15202, OCE78-26820 and OCE76-00596, OCE78-03380 (Coastal Upwelling Ecosystems Analysis (CUEA) program). The authors thank Dr R. Grimshaw for several helpful comments.

## Appendix A. Exponential slope

Approximate solutions to (3.2), (3.3) and (3.5) may be obtained by perturbation methods if it is assumed that $a = H_1/H_2 \ll 1$. Analytical results are obtainable if the slope is assumed to have an exponential form (Buchwald & Adams 1968):

$$H = \exp\left[(\xi - 1)/\delta_B\right]. \tag{A 1}$$

This depth profile, although still highly idealized, is a more realistic model for a continental shelf and slope than the 'weak slope' model used in § 3. The 'weak slope' model is utilized there because the important qualitative features of the solutions are evidently retained while the algebra is considerably simplified. To show that the results are qualitatively similar in the two cases, the solutions for the exponential slope are summarized below. These solutions are also useful to have for estimates of parameter values under oceanic conditions.

Equations (3.2$a, b$) may be written in the form

$$(\phi_{\xi\xi} - \delta_B^{-1}\phi_\xi) + (\delta_B c)^{-1}(f\phi - g) = 0, \tag{A 2a}$$

$$g_{\xi\xi} - (f^2/SH_1)\,g = a[(\delta_B c)^{-1} f(f\phi - g) - \delta_B^{-1} g_\xi + (f^2/SH_1)\,g]. \tag{A 2b}$$

The boundary conditions (3.3$a, b$) and (3.5$a, b$) are

$$\phi = 0, \quad g_\xi + (f/c)\,g = 0 \quad \text{at} \quad \xi = 0, \tag{A 3a, b}$$

$$\phi_\xi = 0, \quad g_\xi + [f(1 + a_{(1)})/SH_1]^{\frac{1}{2}} g = 0 \quad \text{at} \quad \xi = 1. \tag{A 4a, b}$$

For an exponential slope, $\delta_B$ is a constant. We assume that

$$a_{(0)} = H_1/H_{2(0)} \ll 1. \tag{A 5a}$$

In (A 2$b$), we utilize

$$a = H_1/H_2 = a_{(0)} H_{2(0)}/H_2(\xi) = a_{(0)} H_{(0)}/H(\xi) + O(a_{(0)}^2). \tag{A 5b}$$

We also define, for future use,

$$\gamma^2 = f(\delta_B c)^{-1} - \tfrac{1}{4}\delta_B^{-2}. \tag{A 6}$$

Solutions may be obtained following the general procedure used in (3.13)–(3.20). With the variables expanded in the form

$$\phi = \hat{\phi}_n + \ldots, \quad g = a_{(0)}\hat{g}_n + \ldots, \quad c = c_n + \ldots, \tag{A 7a,b,c}$$

the lowest-order approximations to (A 2$a,b$) are

$$\hat{\phi}_{n\xi\xi} - \delta_B^{-1}\hat{\phi}_{n\xi} + (\delta_B c_n)^{-1} f\hat{\phi}_n = 0, \tag{A 8a}$$

$$\hat{g}_{n\xi\xi} - (f^2/\hat{\delta}_R^2)\hat{g}_n = (H_{(0)}/H)(\delta_B c_n)^{-1} f^2 \hat{\phi}_n, \tag{A 8b}$$

and (A 4$b$) becomes

$$\hat{g}_{n\xi} + (f/\hat{\delta}_R)\hat{g}_n = 0 \quad \text{at} \quad \xi = 1, \tag{A 9a}$$

where

$$\hat{\delta}_R^2 = SH_1 = \delta_R^2(1+a) = \delta_{R(0)}^2(1+a_{(0)}). \tag{A 9b}$$

The boundary conditions for (A 8$a,b$) are given by (A 3$a,b$), (A 4$a$), and (A 9$a$). The solution for $\hat{\phi}_n$ is (Buchwald & Adams 1968)

$$\hat{\phi}_n = D_n \exp(\tfrac{1}{2}\xi/\delta_B)\sin k_n\xi, \tag{A 10a}$$

where

$$c_n = f[\delta_B(k_n^2 + \tfrac{1}{4}\delta_B^{-2})]^{-1}, \tag{A 10b}$$

and where $k_n (n = 1, 2, \ldots)$ is the $n$th positive root of

$$\tan k_n = -2\delta_B k_n. \tag{A 10c}$$

The solution for $\hat{g}_n$ is

$$\begin{aligned}\hat{g}_n = D_n[&(\hat{F}\sin\gamma\xi + \hat{G}\cos\gamma\xi)\exp(-\tfrac{1}{2}\xi/\delta_B) + \hat{J}\exp(f(\xi-1)/\hat{\delta}_R)\\ &+ \hat{N}\exp(-f\xi/\hat{\delta}_R)],\end{aligned} \tag{A 10d}$$

where

$$\hat{F} = (\delta_B/\gamma)\hat{I}\hat{G}, \tag{A 10e}$$

$$\hat{G} = f^2(\gamma c)^{-1}[1 + (\delta_B/\gamma)^2\hat{I}^2]^{-1}, \tag{A 10f}$$

$$\hat{J} = -\tfrac{1}{2}(\hat{\delta}_R/f)\exp(-\tfrac{1}{2}\delta_B^{-1})[(\hat{L}\hat{F} - \gamma\hat{G})\sin\gamma + (\gamma\hat{F} + \hat{L}\hat{G})\cos\gamma], \tag{A 10g}$$

$$\hat{I} = [(2\delta_B)^{-2} - \gamma^2 - (f/\hat{\delta}_R)^2], \tag{A 10h}$$

$$\hat{L} = [(f/\hat{\delta}_R) - \tfrac{1}{2}\delta_B^{-1}]. \tag{A 10i}$$

$$\hat{N} = (c - \hat{\delta}_R)^{-1}\{(c\hat{\delta}_R/f)[\hat{F}\gamma - \hat{G}(\tfrac{1}{2}\delta_B^{-1} - fc^{-1})] + \hat{J}(c + \hat{\delta}_R)\exp(-f/\hat{\delta}_R)\}, \tag{A 10j}$$

and where, in (A 10$d$–$j$), $\gamma = k_n$ and $c = c_n$.

Although the cross-shelf structure of $\hat{\phi}_n$ is the same as for barotropic continental-shelf waves, the vertical structure of the resulting velocity field depends on the magnitude of $\hat{\delta}_R$. For $\hat{\delta}_R \ll 1$, the velocity components are essentially barotropic, whereas for $\hat{\delta}_R \gg 1$, $g_\xi \sim -af\phi$, $g + (c/f)g_\xi \sim -af\phi$, and the velocity field is bottom trapped (ageostrophically for $u$).

One additional solution is found with the scaling

$$\phi = \tilde{\phi}_0 + \ldots, \quad g = \tilde{g}_0 + a_{(0)}\tilde{g}_{01} + \ldots, \quad c = c_0 + a_{(0)}c_{01} + \ldots, \tag{A 11a,b,c}$$

in which case (A 2$a,b$) give

$$\tilde{g}_{0\xi\xi} - (f/\hat{\delta}_R)^2\tilde{g}_0 = 0, \tag{A 12a}$$

$$\tilde{\phi}_{0\xi\xi} - \delta_B^{-1}\tilde{\phi}_{0\xi} + (\delta_B c_0)^{-1} f\tilde{\phi}_0 = (\delta_B c_0)^{-1}\tilde{g}_0. \tag{A 12b}$$

The boundary conditions are (A 3$a$, $b$), (A 4$a$) and (A 9$a$). The solution for $\tilde{g}_0$ is the internal Kelvin wave

$$\tilde{g}_0 = C_0 \exp(-f\xi/\hat{\delta}_R), \tag{A 13$a$}$$

where (A 3$b$) implies

$$c_0 = \hat{\delta}_R. \tag{A 13$b$}$$

The solution for $\tilde{\phi}_0$ is

$$\tilde{\phi}_0 = C_0 \hat{E}\{\exp(-f\xi/\hat{\delta}_R) + \exp(\tfrac{1}{2}\xi/\delta_B)[-\cos\gamma\xi + \hat{P}\sin\gamma\xi]\}, \tag{A 13$c$}$$

where

$$\hat{E} = (\delta_B c)^{-1}[(f/\hat{\delta}_R)^2 + f(\hat{\delta}_R\delta_B)^{-1} + f(\delta_B c)^{-1}]^{-1}, \tag{A 13$d$}$$

$$\hat{P} = [(2\delta_B)^{-1}\sin\gamma + \gamma\cos\gamma]^{-1}[(2\delta_B)^{-1}\cos\gamma - \gamma\sin\gamma + (f/\hat{\delta}_R)\exp(-f\hat{\delta}_R^{-1} - \tfrac{1}{2}\delta_B^{-1})], \tag{A 13$e$}$$

and where $\gamma$ is given by (A 6) with $c = c_0$.

The solutions (A 7) and (A 11) are again not valid for parameter values where

$$c_n \simeq c_0. \tag{A 14}$$

In the neighbourhood of these points, the two types of solutions, (A 7) and (A 11), must be considered simultaneously as in (3.22)–(3.32). Approximate solutions for $a_{(0)} \ll 1$, but with no restriction here on the magnitude of $\hat{\delta}_R$, may be written in the form

$$\phi = D\exp(\tfrac{1}{2}\xi/\delta_B)\sin\gamma\xi + C\hat{E}[\exp(-f\xi/\hat{\delta}_R) - \exp(\tfrac{1}{2}\xi/\delta_B)\cos\gamma\xi], \tag{A 15$a$}$$

$$g = C\exp(-f\xi/\hat{\delta}_R) + a_{(0)}D[(\hat{F}\sin\gamma\xi + \hat{G}\cos\gamma\xi)\exp(-\tfrac{1}{2}\xi/\delta_B) + \hat{J}\exp(f(\xi-1)/\hat{\delta}_R)], \tag{A 15$b$}$$

where $\gamma$ is defined in (A 6). The solutions (A 15$a$, $b$) satisfy the boundary conditions (A 3$a$) and (A 9$a$).

Substituting (A 15$a$, $b$) into the two remaining boundary conditions (A 3$b$) and (A 4$a$), we obtain two homogeneous equations for $C$ and $D$ similar to (3.23$a$, $b$). The requirement that these two equations be compatible gives the following equation, analogous to (3.24), for the eigenvalue $c$:

$$(\gamma\cos\gamma + \tfrac{1}{2}\delta_B^{-1}\sin\gamma)(\hat{\delta}_R^{-1} - c^{-1}) = \hat{R}, \tag{A 16$a$}$$

where

$$\hat{R} = a_{(0)}f^{-1}\hat{E}[(f/\hat{\delta}_R)\exp(-\hat{M}) + (\tfrac{1}{2}\delta_B^{-1}\cos\gamma - \gamma\sin\gamma)] \times [\hat{J}f(\hat{\delta}_R^{-1} + c^{-1})\exp(-f/\hat{\delta}_R) + \gamma\hat{F} + (fc^{-1} - \tfrac{1}{2}\delta_B^{-1})\hat{G}], \tag{A 16$b$}$$

and

$$\hat{M} = (f/\hat{\delta}_R) + \tfrac{1}{2}\delta_B^{-1}. \tag{A 16$c$}$$

Similar to (3.25) and (3.26), the solutions for $c$ from (A 16) with $a_{(0)} \ll 1$ may be obtained, for most parameter values, by neglecting $\hat{R}$. This gives $\gamma = k_n$ and $c = c_n$, as in (A 10$b$, $c$), and $c = c_0 = \hat{\delta}_R$ as in (A 13$b$). These solutions are not valid for values of the parameters near points where $c_n \simeq c_0$. To obtain the solutions for $c$ in regions near these points a local analysis is used.

Assume, as in § 3, that the parameter $f$ is variable. Then $c_1 = c_0$ when $f$ has the critical value

$$f_C = \hat{\delta}_R\delta_B(k_1^2 + \tfrac{1}{4}\delta_B^{-2}). \tag{A 17}$$

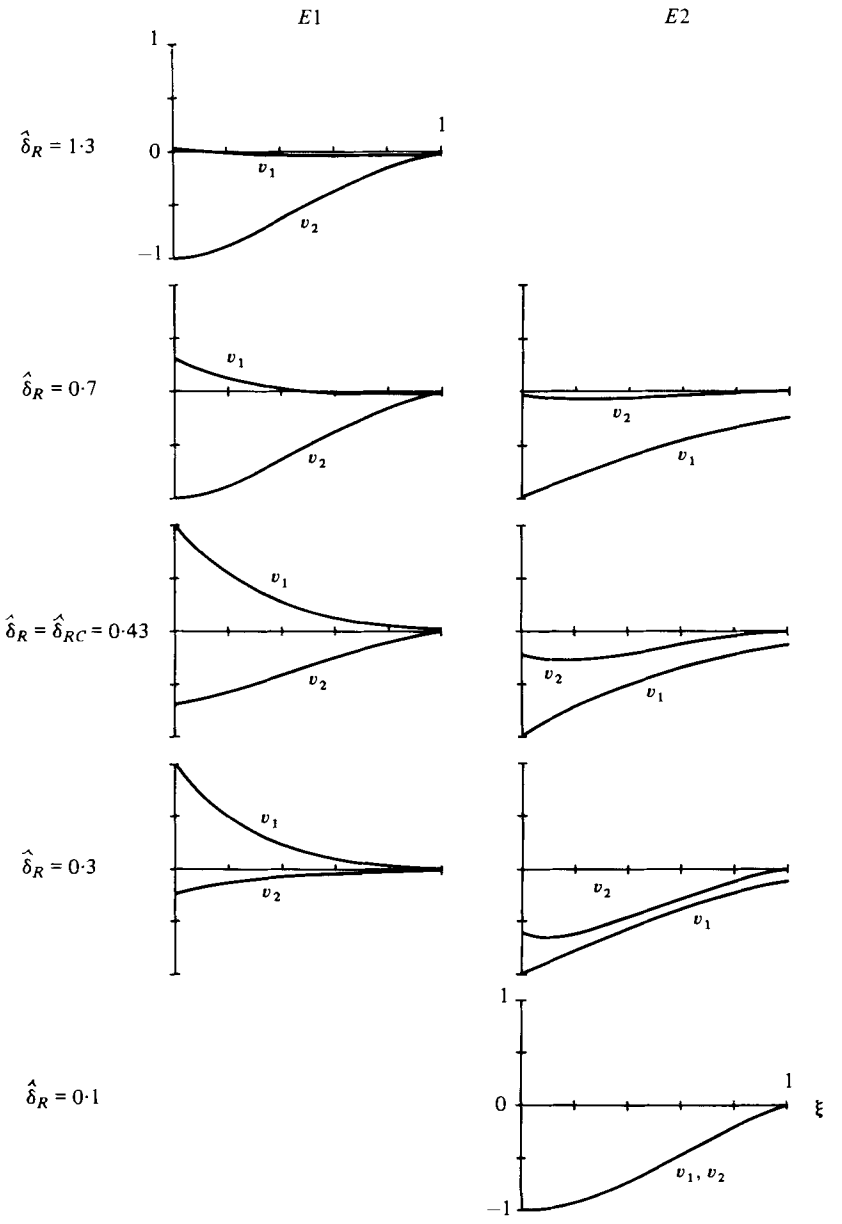


FIGURE 5. The cross-shelf structure of the alongshore velocity components associated with the internal Kelvin wave and the $n = 1$ shelf wave for various values of $f$. The parameter values are discussed in appendix B. Specifically, $a_{(0)} = 0{\cdot}3$, $\delta_B = 0{\cdot}33$, $k_1 = 2{\cdot}18$, $f'_C = 0{\cdot}26 \times 10^{-4}$ s$^{-1}$, $L_s \equiv L_{sC} = 90$ km, $c'_0 = 100$ cm s$^{-1}$. The variation of $f$ is indicated by the variation of $\hat{\delta}_R = c'_0/(f'L_{sC})$, where $\hat{\delta}_R = 0{\cdot}43$ at the critical latitude $f' = f'_C$. For $f' < f'_C (\hat{\delta}_R > \hat{\delta}_{RC})$, the eigenfunction in the left column ($E1$) is the $n = 1$ shelf wave and the eigenfunction in the right column ($E2$) is the internal Kelvin wave. For $\hat{\delta}_R = 1{\cdot}3$, $0{\cdot}7$, $0{\cdot}43$, $0{\cdot}3$, $0{\cdot}1$ the corresponding latitudes are 3·4°, 6·3°, 10·3°, 14·7°, 49·8°, the phase speeds in cm s$^{-1}$ for $E1$ are 33, 59, 85, 97, –, and for $E2$ are –, 103, 114, 147, 430 respectively. The velocities are normalized so that, at $x = 0$, $|\max(v_1, v_2)| = 1$.

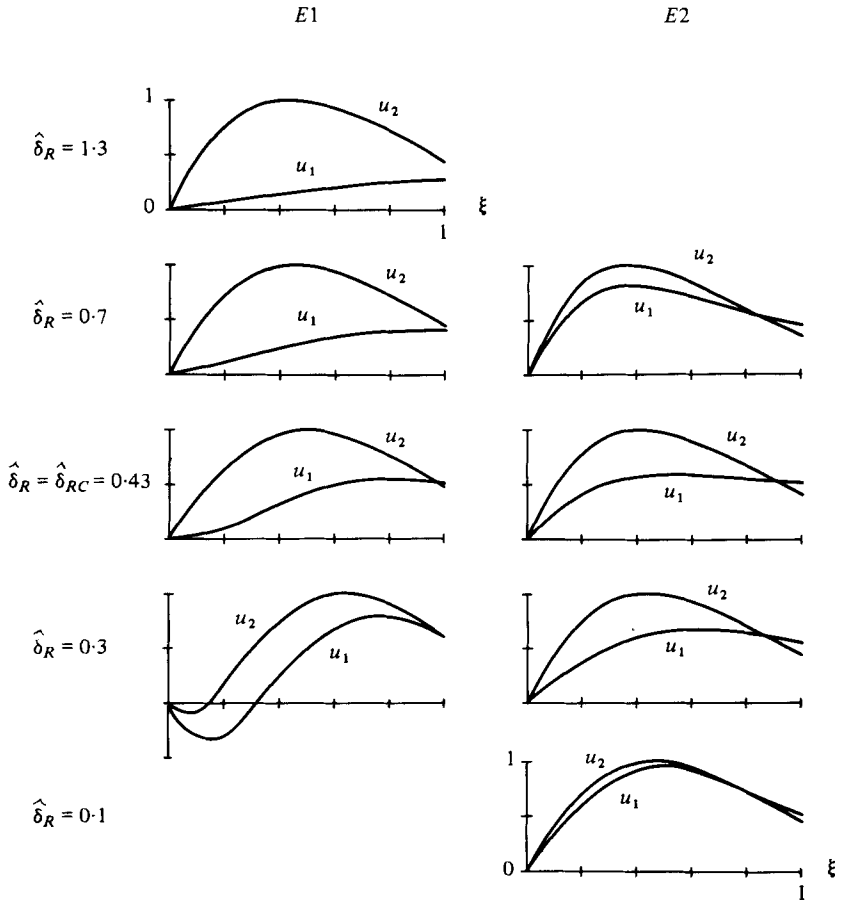


FIGURE 6. The cross-shelf structure of the onshore–offshore velocity components associated with the internal Kelvin wave and the $n = 1$ shelf wave for various values of $f$. The parameters correspond to those in figure 5. The velocities are normalized so $|\max(u_1, u_2)| = 1$.

Solutions for $c$ are sought in the neighbourhood of $f_C$ by expanding $f$ and $c$ as in (3.28), where here $c_C = \hat{\delta}_R$. The approximate solutions for $\tilde{c}$ are given in the form (3.29) where $K \to \hat{K}$ and

$$\hat{K} = \frac{16a_{(0)}(b - \frac{1}{4}\delta_B^{-1})\,[1 - (\delta_B b)^{\frac{1}{2}} \exp(-\hat{M})]^2}{\delta_B^2 b(b + 2\delta_B^{-1})^2 (1 + 2b)}, \tag{A 18a}$$

$$b = f_C/\hat{\delta}_R. \tag{A 18b}$$

The cross-shelf structure of the velocity components associated with the internal Kelvin wave and the $n = 1$ shelf wave are shown in figures 5 and 6 for various values of $f$ less than, equal to and greater than $f_C$. The solutions were calculated from (A 15) and (A 16) using parameter values discussed in appendix B. The change in character of the eigenfunctions as a function of $f$ is clearly illustrated. For $f < f_C$ and $\hat{\delta}_R = 1{\cdot}3,\ 0{\cdot}7$, the $n = 1$ shelf wave is essentially bottom trapped and the internal Kelvin wave has the expected exponential variation in the upper layer, with $v_1 > v_2$ since $a_{(0)} < 1$. In contrast to a flat-bottom internal Kelvin wave, the velocity in the lower layer $v_2$ here is in

the same direction as $v_1$ owing to effects of the bottom topography. At $f = f_C$, $\hat{\delta}_R = 0{\cdot}43$, both eigenfunctions have depth-dependent baroclinic velocities. For $f > f_C$ and $\hat{\delta}_R = 0{\cdot}3$, the eigenfunction, which is the shelf wave for $f < f_C$, has the structure of an internal Kelvin wave whereas the other eigenfunction, which is the internal Kelvin wave for $f < f_C$, has the structure of a shelf wave with weak shear. For $\hat{\delta}_R = 0{\cdot}1$, the latter becomes essentially a depth-independent barotropic shelf wave.

The solutions for $\phi$ and $g$ in (A 15), the solutions for $c$ from (A 16), and the expression for $\hat{K}$ in (A 18) reduce, in the limit $\delta_B \gg 1$, $\hat{\delta}_R \ll 1$, to the appropriate results in § 3.

In connexion with the validity of the slowly-varying approximation, the estimate mentioned after (4.17) of

$$C_{nY}/C_n \simeq \pm 1/(2f_C K^{\frac{1}{2}}), \tag{A 19}$$

gives the following condition, analogous to (4.18), on $|c/\omega|$:

$$|c_C/\omega| \ll f_C \hat{K}/\beta. \tag{A 20}$$

For $a \ll 1$, the internal-Kelvin-wave solution (A 13$a$) is a valid first approximation to one of the solutions to (A 2$a, b$) for all value s of $\hat{\delta}_R$. When $a$ is not small, this is not the case and the equations (A 2$a, b$) may be fully coupled depending on the value of the parameter $\lambda = \delta_{I(0)}/\delta_B$.

In Allen (1975), it was shown, for the exponential slope, that with $\lambda \ll 1$ (actually $a_{(0)}\lambda \ll 1$) (A 2$a, b$) uncouple, so that an internal Kelvin wave with decay scale $\delta_{R(0)}$ is a valid first approximation for one of the solutions. For larger values of $\lambda$, such that $a_{(0)}\lambda^2 \to O(1)$, the equations for $g$ and $\phi$ become fully coupled and the internal Kelvin wave is replaced by a solution of more general form.

In the opposite limit, i.e. where $\delta_R \gg 1$, we expect that an internal Kelvin wave with decay scale $\delta_{R(1)}$ forms a valid first approximation to one of the solutions of (A 2$a, b$). As $\delta_R$ is decreased, however, topographic effects should become important at some point, with the resultant coupling of (A 2$a, b$). The solutions obtained here for small $a$ are useful for demonstrating that the dependence of the coupling of (A 2$a, b$) when $\delta_R$ is large also depends on the parameter $\lambda$. In this case, we find that for $a_{(0)}\lambda^{-2} \ll 1$ the internal Kelvin wave is a valid first approximation, but that, as $\lambda$ decreases so that $a_{(0)}\lambda^{-2} \to O(1)$, topographic effects become important and the equations (A 2$a, b$) become fully coupled.

The parameter dependence of the topographic coupling in (A 2$a, b$) may be illustrated by examining the relative magnitude of $\tilde{g}_0$ and $a_{(0)}\tilde{g}_{01}$ in (A 11$b$). The equation for $\tilde{g}_{01}$ is

$$\tilde{g}_{01\xi\xi} - (f/\hat{\delta}_R)^2 \tilde{g}_{01} = (H_{(0)}/H)\,[(\delta_B c_0)^{-1} f^2 \tilde{\phi}_0 + (f/\hat{\delta}_R)^2 \tilde{g}_0 - \delta_B^{-1}(f c_0^{-1}\tilde{g}_0 + \tilde{g}_{0\xi})], \tag{A 21}$$

with boundary conditions obtained from (A 3$b$) and (A 4$b$) using (A 11$b, c$). We omit the detailed form of the solution for $\tilde{g}_{01}$, but note that the results show

$$a_{(0)}\tilde{g}_{01}/\tilde{g}_0 \simeq a_{(0)}\lambda^2 \quad \text{for} \quad a_{(0)}\lambda^2 < 1, \tag{A 22$a$}$$

$$a_{(0)}\tilde{g}_{01}/\tilde{g}_0 \simeq a_{(0)}\lambda^{-2} \quad \text{for} \quad a_{(0)}\lambda^{-2} < 1. \tag{A 22$b$}$$

Since (A 2$a, b$) are coupled for $a_{(0)}\hat{g}_{01}/\hat{g}_0 = O(1)$, (A 22$a, b$) exhibit the coupling dependence on $\lambda$.

Insight into the way in which (A 22$a, b$) arise may be obtained from rough order-of-magnitude estimates. Assuming for the exponential slope that $\delta_B < 1$, we may estimate from (A 12$b$) that

$$\tilde{\phi}_0 \simeq \delta_\xi^2(\delta_B \hat{\delta}_R)^{-1}\tilde{g}_0. \tag{A 23$a$}$$

Utilizing (A 23$a$) in (A 21), we obtain

$$\tilde{g}_{01} \simeq \delta_\xi^4(\delta_B \hat{\delta}_R)^{-2}\tilde{g}_0. \tag{A 23$b$}$$

A choice for $\delta_\xi$ which is consistent with (A 23$a, b$) is

$$\delta_\xi \simeq \min(\hat{\delta}_R, \delta_B). \tag{A 24}$$

The use of (A 24) in (A 23$b$) gives the results (A 22$a, b$) in the appropriate limits.

## Appendix B. Parameter values

For an estimate of parameter values under oceanic conditions, we use the results in appendix A from the exponential slope model with $a_{(0)} \ll 1$. We restrict our attention to the low-latitude region of the eastern Pacific Ocean, south of the equator, off South America.

Dimensional local values of the wave speed of the first ($n = 1$) shelf-wave solution as a function of latitude may be roughly estimated by using (A 10$b$) and the values of the shelf-slope width in table 1. Recall that, under the assumption $a_{(0)} \ll 1$, this relation gives a valid first approximation to the shelf-wave speed regardless of the relative magnitude of the internal Rossby radius of deformation and the shelf-slope width or, more precisely, independent of the value of $\lambda = \delta_{R(0)}/\delta_B$.

We use a constant value of $\delta_B = 0{\cdot}33$, which corresponds to the assumption that in the exponential slope model the ratio of the depth at the coast $H'_{(0)}$ to the depth at the slope-interior junction $H'_0$ has a fixed value of $H'_{(0)}/H'_0 = 0{\cdot}05$. This is satisfied, for example by $H'_{(0)} = 180\,\text{m}$ and $H'_0 = 3650\,\text{m}$. The dimensional value of $\delta_B$ is then given by $\delta'_B = \delta_B L_s$. With $\delta_B$ specified, the solution of (A 10$c$) gives $k_1 = 2{\cdot}18$. The dimensional value of the $n = 1$ shelf wave speed, from (A 10$b$), is

$$c'_1 = f' L_s[\delta_B(k_1^2 + \tfrac{1}{4}\delta_B^2)]^{-1}, \tag{B 1}$$

where $f'$ is the dimensional Coriolis parameter. Values of $\delta'_B$ and $c'_1$, calculated using the appropriate local values of $f'$ and $L_s$, are given in table 1.

The wave speed of the internal Kelvin wave in the region of interest is estimated to be $c'_0 = 100\,\text{cm s}^{-1}$ (based on $\Delta\rho/\rho_2 \simeq 1{\cdot}5 \times 10^{-3}$ and $H'_1 = 70\,\text{m}$). It may be seen from the values of $c'_1$ in table 1 that, as the latitude increases, $c'_1$ increases so that $c'_1 \simeq c'_0$ first at some location between 10° and 11° S. We use that critical latitude for further estimates of parameter values.

For $c'_1 = 100\,\text{cm s}^{-1}$, (B 1) implies that $f'_C L_{sC} = 233\,\text{cm s}^{-1}$, which should hold at some particular latitude between 10° and 11° S. If we assume $L_{sC} = 90\,\text{km}$, which is between the values of $L_s$ at 10° and 11°, we obtain $f'_C = 0{\cdot}259 \times 10^{-4}\,\text{s}^{-1}$. This value of $f'_C$ corresponds to a latitude of 10° 15′ S.

With $\beta' = 2{\cdot}26 \times 10^{-13}\,\text{cm}^{-1}\,\text{s}^{-1}$, (A 20) gives a restriction on the wavelength in the $y$ direction, $\delta_y = 2\pi c/\omega$, such that the slowly-varying approximation is valid. In terms of dimensional values, (A 20) implies

$$\delta'_y \ll L_V = (2\pi f'_C/\beta')\,\hat{K}. \tag{B 2}$$

| | |
|---|---|
| $\delta_B = 0{\cdot}33$ | $\beta' = 2{\cdot}26 \times 10^{-13}$ cm$^{-1}$ s$^{-1}$ |
| $k_1 = 2{\cdot}18$ | $f'_C/\beta' = 1\,150$ km |
| $c'_0 = 100$ cm s$^{-1}$ | $\hat{K} = 0{\cdot}241 a_{(0)}$ |
| $f'_C L_{sC} = 233$ cm s$^{-1}$ | $L_V = 1100$ km |
| $f'_C = 0{\cdot}259 \times 10^{-4}$ s$^{-1}$ | |

TABLE 2. Summary of parameter values estimated in appendix B.

Evaluating $\hat{K}$ from (A 18) with $f_C/\delta_R = f'_C L_{sC}/c'_0 = 2{\cdot}33$, we obtain $\hat{K} = 0{\cdot}241 a_{(0)}$. Although the determination of $\hat{K}$ was based on the approximation $a_{(0)} \ll 1$, for an estimation of $\delta_y$ we use $a_{(0)} = 0{\cdot}64$, corresponding to the observed pycnocline depth of $H'_1 = 70$ m and to $H'_{(0)} = 180$ m. This gives $L_V = 1100$ km which is discussed in § 5.

In the plots of eigenfunctions in figures 5 and 6, however, we choose a smaller value for $a_{(0)}$, i.e. $a_{(0)} = 0{\cdot}3$, but we keep $c'_0 = 100$ cm s$^{-1}$, so that, with $H'_{(0)} = 180$ m, this case corresponds to $H'_1 = 41$ m and $\Delta\rho/\rho_2 = 2{\cdot}5$. A summary of parameter values is given in table 2.

We note that the internal Kelvin wave speed $c'_0 = 100$ cm s$^{-1}$ and the shelf-wave speeds in table 1 at the appropriate latitudes are substantially less than the value of 230 cm s$^{-1}$ observed by Smith (1978) between 10° and 15° S off Peru. The reasons for this lack of quantitative agreement are not completely understood, but are probably due to inadequacies of the two-layer model in representing the coastal trapped waves in that location.

The estimated value of $\delta_{E1} \simeq 260$ km for a two-layer model of the eastern equatorial Pacific Ocean, given in § 1, follows from the assumption, based on data from Wyrtki (1964), that at 115° W $\Delta\rho/\rho_2 \simeq 2{\cdot}5 \times 10^{-3}$ and $H'_1 = 100$ m, which gives

$$H_{e1} = (\Delta\rho/\rho_2) H'_1 H'_2/(H'_1 + H'_2) \simeq 25 \text{ cm}.$$

## Appendix C. Mechanical analogy

A simple mechanical system with a behaviour similar to that found for the waves in § 3 is provided, as noted by Garrett (1969), by two weakly-coupled linear harmonic oscillators. This analogy may also be extended to the case of a slowly varying environment, such as in § 4.

Consider two weakly coupled pendulums. There are two normal modes of oscillation. For pendulums of different length, one mode will have energy primarily in one pendulum, with a modal frequency close to the natural frequency of that pendulum, and the second mode will have energy primarily in the other pendulum. If the lengths of the pendulums are varied, so that the long pendulum becomes the short one, and if the modes are identified as continuous functions of the lengths, it is found that the structure of each mode changes so that the concentration of energy switches to the other pendulum. When the lengths are equal, the energy in each mode is equally partitioned between the two pendulums. This behaviour is depicted in figure 7. The analogy with the behaviour of waves in § 3 follows from the identification of changes in length of the pendulums with changes in $f$ and of oscillations is a particular pendulum with the motion in a particular type of wave. The situation where the pendulums have equal lengths corresponds, of course, to $f = f_C$.

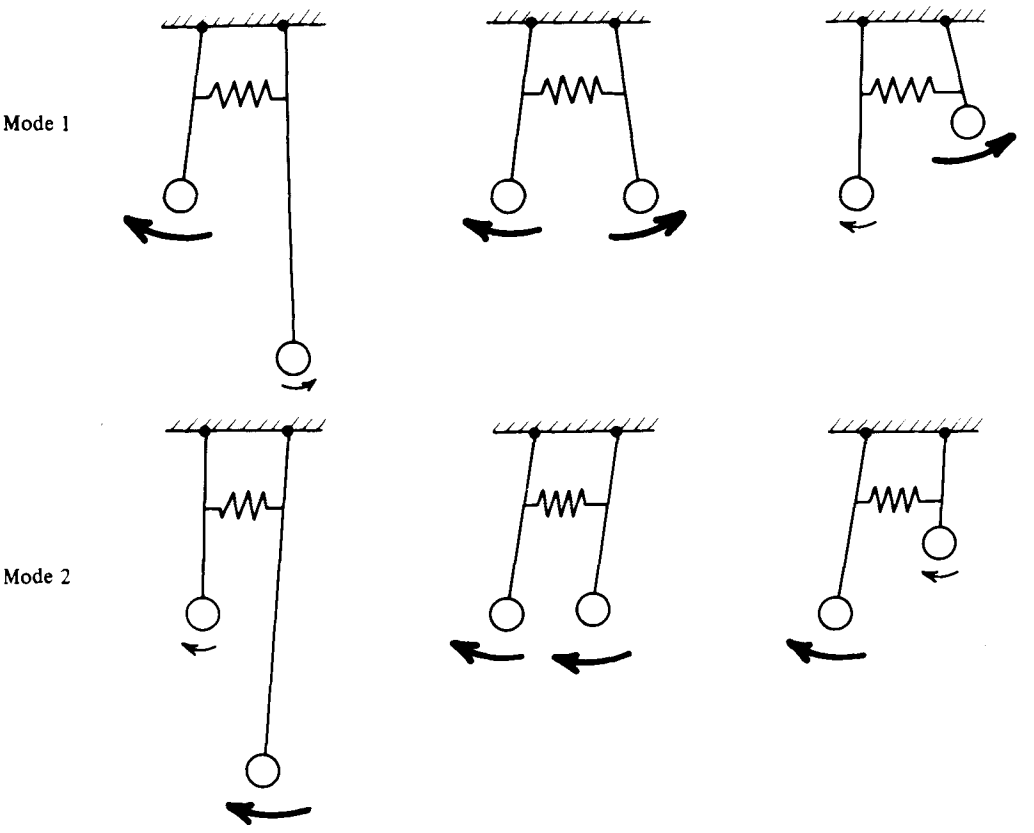


FIGURE 7. Schematic diagram of the behaviour of the two normal modes of oscillation of two linear, weakly coupled pendulums as the relative lengths of the pendulums are varied. The magnitudes of the arrows indicate the relative concentration of energy in each pendulum.

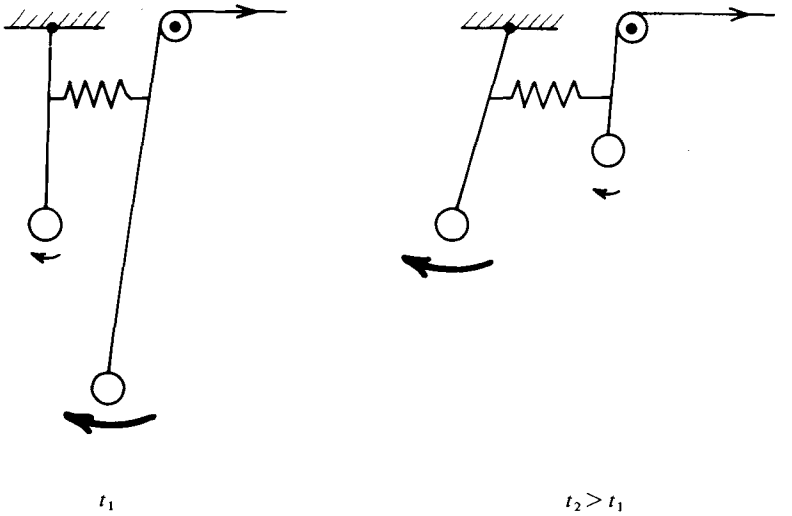


FIGURE 8. Schematic of the behaviour in time of the oscillations in a problem where the length of the pendulum on the right is varied slowly and where the oscillations are started initially with energy only in one mode (i.e. mode 2, from figure 7).

To extend the analogy to the case of a slowly varying environment as in § 4, consider a problem where the lengths of the pendulums are varied slowly. A WKB type of analysis of the governing equations for this system, outlined below, shows that the action in each mode, where the action is the energy in the mode divided by the frequency, is conserved provided the variations are slow enough. In that case, if oscillations are started with energy in one mode and with no energy in the other mode, only the mode with initial energy will be present at later times.

Consider a situation, therefore, where the oscillations are started in only one mode and where, for example, the length is varied so that the initially longer pendulum becomes the short pendulum. A problem of this type is illustrated in figure 8. Since the oscillations remain only in the initially excited mode, the concentration of energy switches from one pendulum to the other as the length varies past the point of equal lengths. The analogy of the behaviour in this problem with that of the waves in § 4 follows immediately from the same identification of waves and pendulums noted above.

It is useful to outline briefly an analysis of the coupled, slowly varying pendulum problem which parallels that in § 4 and which establishes in a similar manner the condition, analogous to (4.18), that the slowly-varying approximation remains valid. This condition may then be compared with the results from a more complete asymptotic analysis of linearly coupled, slowly varying oscillators by Grimshaw & Allen (1979). The governing equations are assumed to be

$$y_{1tt} + \lambda_1^2(T)\, y_1 = 2\mu\lambda^2 y_2, \tag{C 1a}$$

$$y_{2tt} + \lambda_2^2(T)\, y_2 = 2\mu\lambda^2 y_1, \tag{C 1b}$$

where $T = \epsilon t$, $\lambda_1(0) = \lambda_2(0) = \lambda$, $\epsilon \ll 1$, and $\mu \ll 1$. Solutions are sought in the form

$$[y_1, y_2] = \mathrm{Re}\left\{[A(T), B(T)] \exp\left(i\epsilon^{-1}\int_0^T \omega\, dT'\right)\right\}. \tag{C 2}$$

Substituting (C 2) in (C 1) and expanding $A = A_0 + \epsilon A_1 + \ldots$, $B = B_0 + \epsilon B_1 + \ldots$, we obtain

$$(\omega^2 - \lambda_1^2) A_0 + 2\mu\lambda^2 B_0 = 0, \tag{C 3a}$$

$$2\mu\lambda^2 A_0 + (\omega^2 - \lambda_2^2) B_0 = 0, \tag{C 3b}$$

$$(\omega^2 - \lambda_1^2) A_1 + 2\mu\lambda^2 B_1 = i(2A_{0T}\omega + A_0\omega_T), \tag{C 4a}$$

$$2\mu\lambda^2 A_1 + (\omega^2 - \lambda_2^2) B_1 = i(2B_{0T}\omega + B_0\omega_T). \tag{C 4b}$$

From (C 3$a, b$) we find

$$\omega_\pm^2 = \tfrac{1}{2}(\lambda_1^2 + \lambda_2^2) \pm \tfrac{1}{2}[(\lambda_1^2 - \lambda_2^2)^2 + 16\mu^2\lambda^4]^{\frac{1}{2}}, \tag{C 5}$$

which for $T/\mu \ll 1$ gives

$$\omega_\pm^2 = \lambda^2 + \lambda T(\lambda_1' + \lambda_2') \ldots \pm 2\mu\lambda^2[1 + (\lambda_1' - \lambda_2')^2 (2\mu\lambda)^{-2} T^2 + \ldots]^{\frac{1}{2}}, \tag{C 6}$$

where $\lambda_{1,2}' = \lambda_{1,2T}(0)$.

The compatibility condition for (C 4$a, b$) is

$$(\omega^2 - \lambda_1^2)(2B_{0T}\omega + B_0\omega_T) - 2\mu\lambda^2(2A_{0T}\omega + A_0\omega_T) = 0. \tag{C 7}$$

With $(A_0, B_0) = (a, b)\exp(i\chi)$, (C 7) and (C 3$a, b$) imply

$$[(a^2 + b^2)\omega]_T = [\mathscr{E}/\omega]_T = 0, \quad \chi_T = 0, \tag{C 8a, b}$$

where $\mathscr{E} = (a^2+b^2)\omega^2$. Relation (C 8$a$), of course, is analogous to (4.10$b$) and expresses the conservation of action $\mathscr{E}/\omega$ for each mode.

To check the validity of (C 3), (C 4) and (C 8) near $T = 0$ we examine the ratio of neglected to retained terms in (C 3), for example

$$R = \frac{2\epsilon A_{0T}\omega}{A_0(\omega^2-\lambda_1^2)} \quad \text{at} \quad T = 0. \tag{C 9}$$

It follows from (C 6) and the definition of $A_0$ that

$$R \simeq 2\epsilon(2\mu\lambda)^{-1}(a_T/a)_{(0)}, \tag{C 10}$$

where $(a_T/a)_{(0)} = a_T(0)/a(0)$. A determination of $(a_T/a)_{(0)}$ using (C 8) gives

$$(a_T/a)_{(0)} = \tfrac{1}{2}(2\mu\lambda)^{-1}(\lambda_1'-\lambda_2'). \tag{C 11}$$

Note that approximating $(a_T/a)_{(0)} \simeq 1/(2\Delta T)$ and estimating $\Delta T \simeq 2\mu\lambda/(\lambda_1'-\lambda_2')$ from (C 6) also gives (C 11). As a result,

$$R \simeq \epsilon|\lambda_1'-\lambda_2'|/(2\mu\lambda)^2. \tag{C 12}$$

For $R \ll 1$, the slowly-varying approximation remains valid in the neighbourhood of $T = 0$, equations (C 3$a$, $b$) and (C 8) determine the lowest-order approximate solution and the action in each mode is conserved. Since $2\mu\lambda = \Delta\omega_{(0)} = (\omega_+-\omega_-)_0$, (C 12) is clearly analogous to (4.20).

In the analysis of Grimshaw & Allen (1979), a multiple-time scale asymptotic procedure is used to derive equations which describe the possible mode coupling near $T = 0$. These equations are solved exactly. It is found that the strength of the mode coupling depends on the parameter $R$ in (C 12). For $R \ll 1$, the amount of action exchanged between modes is exponentially small. In fact, for the problem described in figure 8, where all the action is initially in one mode, most of the action ($\frac{4}{5}$) is retained in that mode even if $R = 1$.

It seems likely that the analysis in Grimshaw & Allen (1979) may be extended to the wave problem in § 4 and that a similar result will follow. The extended analysis would probably show, as in the oscillator case, that most of the energy would remain in the originally excited eigenfunction even if $\delta_y' \simeq L_V$.

## REFERENCES


Allen, J. S. 1975 Coastal trapped waves in a stratified ocean. *J. Phys. Oceanog.* **5**, 300–325.

Anderson, D. L. T. & Rowlands, P. B. 1976 The role of inertia-gravity and planetary waves in the response of a tropical ocean to the incidence of an equatorial Kelvin wave on a meridional boundary. *J. Mar. Res.* **34**, 395–417.

Bretherton, F. P. 1968 Propagation in slowly varying waveguides. *Proc. Roy. Soc.* A **302**, 555–576.

Brink, K. H., Allen, J. S. & Smith, R. L. 1978 A study of low-frequency fluctuations near the Peru coast. *J. Phys. Oceanog.* **8**, 1025–1041.

Buchwald, V. T. & Adams, J. K. 1968 The propagation of continental shelf waves. *Proc. Roy. Soc.* A **305**, 235–250.

Cane, M. A. & Sarachik, E. S. 1976 Forced baroclinic ocean motions: I. The linear equatorial unbounded case. *J. Mar. Res.* **34**, 629–665.

Cane, M. A. & Sarachik, E. S. 1977 Forced baroclinic ocean motions. II. The linear equatorial bounded case. *J. Mar. Res.* **35**, 395–432.

GARRETT, C. J. R. 1969 Atmospheric edge waves. *Quart. Jl R. Met. Soc.* **95**, 731–753.

GILL, A. E. & SCHUMANN, E. H. 1974 The generation of long shelf waves by wind. *J. Phys. Oceanog.* **4**, 83–90.

GRIMSHAW, R. 1977 The effects of a variable Coriolis parameter, coastline curvature and variable bottom topography on continental-shelf waves. *J. Phys. Oceanog.* **7**, 547–554.

GRIMSHAW, R. & ALLEN, J. S. 1979 Linearly coupled, slowly varying oscillators. *Stud. appl. Math.* **66**, 51–71.

HURLBURT, H. E., KINDLE, J. C. & O'BRIEN, J. J. 1976 A numerical simulation of the onset of El Niño. *J. Phys. Oceanog.* **6**, 621–631.

HUYER, A., HICKEY, B. M., SMITH, J. D. & PILLSBURY, R. D. 1975 Alongshore coherence at low frequencies in currents observed over the continental shelf off Oregon and Washington. *J. Geophys. Res.* **80**, 3495–3505.

INCE, E. L. 1956 *Ordinary Differential Equations*, p. 205. Dover.

KUNDU, P. K. & ALLEN, J. S. 1976 Some three-dimensional characteristics of low-frequency current fluctuations near the Oregon Coast. *J. Phys. Oceanogr.* **6**, 181–199.

LIGHTHILL, J. J. 1969 Dynamic response of the Indian Ocean to the onset of the Southwest Monsoon. *Phil. Trans. Roy. Soc.* A **265**, 45–92.

MCCREARY, J. 1976 Eastern tropical ocean response to changing wind systems with application to El Niño. *J. Phys. Oceanog.* **6**, 632–645.

MILES, J. W. 1972 Kelvin waves on oceanic boundaries. *J. Fluid Mech.* **55**, 113–127.

MOORE, D. W. 1968 Planetary-gravity waves in an equatorial ocean. Ph.D. thesis, Harvard University.

MOORE, D. W. & PHILANDER, S. G. H. 1977 Modeling of the tropical ocean circulation. *The Sea*, vol. VI (ed. E. D. Goldberg *et al.*), cha. 8. Wiley-Interscience.

RHINES, P. 1970 Edge, bottom and Rossby waves in a rotating stratified fluid. *Geophys. Fluid Dyn.* **1**, 273–302.

SMITH, R. L. 1978 Poleward propagating perturbations in sea level and currents along the Peru coast. *J. Geophys. Res.* **83**, 6083–6092.

WANG, D. P. & MOOERS, C. N. K. 1976 Coastal trapped waves in a continuously stratified ocean. *J. Phys. Oceanog.* **6**, 853–863.

WYRTKI, K. 1964 The thermal structure of the Eastern Pacific Ocean. *Dt. hydrogr. Z., Ergan-zungsh.* A **6**.